creative commons
COMMONS DEED

저작자표시-비영리-변경금지 2.0 대한민국

이용자는 아래의 조건을 따르는 경우에 한하여 자유롭게

- 이 저작물을 복제, 배포, 전송, 전시, 공연 및 방송할 수 있습니다.

다음과 같은 조건을 따라야 합니다:

저작자표시. 귀하는 원저작자를 표시하여야 합니다.

비영리. 귀하는 이 저작물을 영리 목적으로 이용할 수 없습니다.

변경금지. 귀하는 이 저작물을 개작, 변형 또는 가공할 수 없습니다.

- 귀하는, 이 저작물의 재이용이나 배포의 경우, 이 저작물에 적용된 이용허락조건을 명확하게 나타내어야 합니다.
- 저작권자로부터 별도의 허가를 받으면 이러한 조건들은 적용되지 않습니다.

저작권법에 따른 이용자의 권리는 위의 내용에 의하여 영향을 받지 않습니다.

이것은 이용허락규약(Legal Code)을 이해하기 쉽게 요약한 것입니다.

Disclaimer

dCollection

연세대학교
YONSEI UNIVERSITY

Lactobacillus acidophilus KBL409 protects against kidney injury via improving mitochondrial function in mice with chronic kidney disease

Ki Heon Nam

Department of Medicine

The Graduate School, Yonsei University

연세대학교
YONSEI UNIVERSITY

Lactobacillus acidophilus KBL409 protects against kidney injury via improving mitochondrial function in mice with chronic kidney disease

Directed by Professor Seung Hyeok Han

The Doctoral Dissertation
submitted to the Department of Medicine,
the Graduate School of Yonsei University
in partial fulfillment of the requirements for the degree of
Doctor of Philosophy

Ki Heon Nam

June 2022

연세대학교
YONSEI UNIVERSITY

This certifies that the Doctoral Dissertation of
Ki Heon Nam is approved.

Thesis Supervisor : Seung Hyeok Han

Thesis Committee Member##1 : Jung Tak Park

Thesis Committee Member##2 : Hyoungnae Kim

Thesis Committee Member##3 : Beom Jin Lim

Thesis Committee Member##4 : Je-Wook Yu

The Graduate School
Yonsei University

June 2022

연세대학교
YONSEI UNIVERSITY

ACKNOWLEDGEMENTS

First and foremost, I would like to express my deepest appreciation to my supervisor Prof. Seung Hyeok Han for his continuous support and cheerful enthusiasm. His guidance and advice carried me through every stage of writing this thesis. I could not imagine having a better advisor and mentor for my research.

I am also sincerely grateful to Prof. Jung Tak Park, Prof. Hyoungnae Kim, Prof. Beom Jin Lim, and Prof. Je-Wook Yu for their thoughtful advice and helpful instruction that taught me so much. I would also like to extend my gratitude to Dr. Jimin Park and Dr. Bo Young Nam for their efforts and sacrifices. They supported me in every step of my experimentation. I would also like to give my sincere thanks to Prof. Shin-Wook Kang for his endless support and encouragement.

I also know I could not have accomplished this research without my family's love and support. I owe huge thanks to my parents for the endless love they have given me throughout my life. I also sincerely appreciate my mother-in-law for her unconditional support and love. Finally, I would like to dedicate this thesis to my beloved wife and sons who always bring me joy. Without you, none of this would have been possible.

연세대학교
YONSEI UNIVERSITY

<TABLE OF CONTENTS>

연세대학교
YONSEI UNIVERSITY

연세대학교
YONSEI UNIVERSITY

LIST OF FIGURES

연세대학교
YONSEI UNIVERSITY

LIST OF TABLES

연세대학교
YONSEI UNIVERSITY

ABSTRACT

Lactobacillus acidophilus KBL409 protects against kidney injury via improving mitochondrial function in mice with chronic kidney disease

Ki Heon Nam

Department of Medicine
The Graduate School, Yonsei University

(Directed by Professor Seung Hyeok Han)

Background: Recent advances have led to greater recognition of the role of mitochondrial dysfunction in the pathogenesis of chronic kidney disease (CKD). There has been evidence that CKD is also associated with dysbiosis. Here, I aimed to evaluate whether probiotic supplements can have protective effects against kidney injury via improving mitochondrial function.

Methods: An animal model of CKD was induced by feeding C57BL/6 mice a diet containing 0.2% adenine. KBL409, a strain of *Lactobacillus acidophilus*, was administered via oral gavage at a dose of 1×10^9 CFU daily. To clarify the underlying mechanisms by which probiotics exert protective effects on mitochondria in CKD, primary mouse tubular epithelial cells stimulated with TGF-β and p-cresyl sulfate were administered with butyrate.

Results: In CKD mice, PGC-1α and AMPK, key mitochondrial energy metabolism regulators, were down-regulated. In addition, mitochondrial dynamics shifted toward fission, the number of fragmented cristae increased, and mitochondrial mass decreased. These alterations were restored by KBL409 administration. KBL409 supplementation

연세대학교
YONSEI UNIVERSITY

also improved defects in fatty acid oxidation and glycolysis and restored the suppressed enzyme levels involved in TCA cycle. Accordingly, there was a concomitant improvement in mitochondrial respiration and ATP production assessed by mitochondrial function assay. These favorable effects of KBL409 on mitochondria ultimately decreased kidney fibrosis in CKD mice. *In vitro* analyses with butyrate recapitulated the findings of animal study.

Conclusions: This study demonstrates that administration of the probiotic *Lactobacillus acidophilus* KBL409 protects against kidney injury via improving mitochondrial function.

Key words: probiotics, KBL409, mitochondria, chronic kidney disease

연세대학교
YONSEI UNIVERSITY

Lactobacillus acidophilus KBL409 protects against kidney injury via improving mitochondrial function in mice with chronic kidney disease

Ki Heon Nam

Department of Medicine
The Graduate School, Yonsei University

(Directed by Professor Seung Hyeok Han)

I. INTRODUCTION

Mitochondria are membrane-bound cell organelles that produce most of the chemical energy in mammalian cells. Apart from their crucial respiratory function, mitochondria also play a key role in regulating a variety of cellular processes including cell signaling, maintaining homeostasis of intracellular calcium, inflammation, and cell death pathway. The kidney is enriched in mitochondria because it consumes a large amount of energy and so engages in related activities, including the reabsorption of glucose, sodium, and nutrients in the proximal tubules.[1,2] Given its high oxygen and energy requirements, the homeostasis and viability of the kidney cells are closely associated with mitochondrial function. Thus, dysregulated mitochondria have gained recognition in the pathogenesis of both acute kidney injury and chronic kidney disease (CKD).[3,4] Mitochondrial dysfunction occurs in the early phase of kidney injury and is closely linked with the development and progression of CKD.[4-7] The hallmark features of mitochondrial dysfunction are increased mitochondrial fragmentation, mitochondrial remodeling, increased oxidative stress, and decreased ATP production.[4,8] Such altered mitochondria eventually lead to inflammation, cell injury, and death.[9] Therefore, there has

연세대학교
YONSEI UNIVERSITY

been an increasing need for new therapeutic strategies targeting mitochondria protection in the context of kidney failure.[7,10,11] Of note, preclinical studies have shown the renoprotective effects of mitochondria-targeted approaches, including mitochondrial-specific antioxidants,[12-14] and various agents that regulate mitochondrial fatty acid oxidation (FAO),[15,16] biogenesis,[17,18] and dynamics.[19] However, the therapeutic efficacy of mitochondria-protecting drugs has not yet been proven in clinical practice.

Normal gut microbiota plays an important role in nutrient and drug metabolism, maintenance of structural integrity of the gut mucosal barrier, immunomodulation, and protection against enteric pathogens.[20] Healthy gut microbiota is largely responsible for overall health. Interestingly, the intestinal microbiome is markedly altered to an imbalance state, so-called dysbiosis, in patients with CKD.[21] Dysbiosis contributes to increase in the production of gut-derived uremic toxins and intestinal permeability, both of which facilitate the translocation of toxins and bacteria into the blood resulting in inflammation and kidney injury.[22] In this regard, many experimental studies to date have shown the beneficial effects of probiotics against kidney injury.[23-27] Potential mechanisms of probiotics involve improving gut permeability, decreasing inflammation and oxidative stress, reducing uremic toxin, and increasing the production of beneficial short-chain fatty acids (SCFAs), metabolites of intestinal bacteria.[21,24-27] However, it is unknown whether probiotics can improve impaired mitochondrial dynamics and metabolism during kidney failure. Notably, previous experimental and human studies have demonstrated the potential beneficial effects of probiotics on mitochondria in many cell types such as enterocytes, hepatocytes, and cardiomyocytes.[28-31] In addition, SCFAs ameliorated hypoxia-induced injury in kidney tubular epithelial cells (TECs) by improving mitochondrial biogenesis.[23] SCFAs also affect energy homeostasis and metabolism by

연세대학교
YONSEI UNIVERSITY

regulating mitochondrial functions and dynamics in brown adipocytes, and liver, skeletal muscle, pancreatic β-cells.[32-35]

Therefore, in this study, I hypothesized that administering probiotics would have renoprotective effects by improving mitochondrial function in an animal model of kidney injury. I also examined how SCFAs affected mitochondria in kidney TECs.

II. MATERIALS AND METHODS

1. Selection of probiotics

Probiotics that can decompose p-cresol were screened by my collaborators (KoBioLabs, Inc., Seoul, South Korea). They tested 67 human-derived *Lactobacillus* and *Lactococcus* strains and 33 *Bifidobacterium* strains. Using gas chromatography (GC-EI-MS, Agilent Technologies, Santa Clara, CA, USA), p-cresol decomposition was determined by measuring the concentration of p-cresol remaining after culturing the strains in MRS medium containing p-cresol. In this study, I selected KBL409, a strain of *Lactobacillus acidophilus*, for experimentation because it showed greater ability to decompose p-cresol than the other tested strains.[36]

2. Animal model

All animal experiments were conducted following a protocol approved by the Committee for the Care and Use of Laboratory Animals of Yonsei University College of Medicine. In this study, I used a CKD model that was induced by feeding six-week-old C57BL/6J mice a 0.2% adenine-containing diet.[37] The mice were randomly assigned to one of four groups: control + phosphate-buffered saline (PBS), control + KBL409, CKD + PBS, and CKD + KBL409. *Lactobacillus acidophilus* KBL409 was administered via

연세대학교
YONSEI UNIVERSITY

oral gavage at a dose of 1×10^9 colony-forming units once daily for 3 weeks, after which all mice were sacrificed.

3. Quantification of SCFAs in cecum samples

To measure SCFA levels in cecum samples, ceca were homogenized in distilled water and centrifuged at 13,000 × g for 5 minutes. The supernatant was collected and an internal standard of 1% 2-methylpentanoic acid was added. Next, ethyl ether was added to the solution as an extraction solvent and then the solution was centrifuged at 13,000 × g for 5 minutes. The organic layers of samples were analyzed using an Agilent 7890A gas chromatograph (Agilent Technologies, Santa Clara, CA, USA) under the following conditions: a capillary voltage of 1.5 kV, a desolvation gas flow of 600 L h^{-1}, a cone gas flow of 50 L h^{-1}, an oven temperature of 170℃ and flame ionization detector and injection port temperature of 225℃. The samples' times and peak areas were measured using a standard mixture.

4. Primary culture of kidney tubular epithelial cells

Kidney TECs were isolated from C57BL/6J mice and cultured in the Dulbecco's Modified Eagle Medium (DMEM) (Gibco, Thermo Fisher Scientific, Waltham, MA, USA) containing 10% fetal bovine serum (FBS) (Thermo Fisher Scientific, Waltham, MA, USA), 100 U/ml penicillin G, 2.5 μg/ml amphotericin B, and 20 ng/ml epidermal growth factor (all from Sigma Aldrich, St. Louis, MO, USA). Kidneys were dissected, placed in 1 ml ice-cold Dulbecco's phosphate buffered saline (DPBS) containing collagenase and digested for 60 minutes at 37℃. The supernatant was then sieved through a nylon mesh and the obtained samples were centrifuged for 10 minutes at 3,000

연세대학교
YONSEI UNIVERSITY

rpm. Pellets were resuspended in 5 ml sterile red blood cell lysis buffer and kept at 4℃ for 3 minutes, then centrifuged for 10 minutes at 3,000 rpm. The pellet was washed twice with DPBS and seeded in culture dishes. To induce cell injury under conditions similar to kidney failure, primary TECs were cultured in medium with 10 ng/ml transforming growth factor-β (TGF-β) and 0.5 mM p-cresyl sulfate (PCS). The protective effect of SCFAs under uremic conditions was evaluated using 10 mM butyrate (Sigma-Aldrich, St. Louis, MO, USA). The cells were maintained at 37℃ in a humidified 5% CO_2 incubator and harvested after 48 hr of stimulation.

5. Total RNA extraction

Whole kidney samples were rapidly frozen using liquid nitrogen and homogenized by mortar and pestle 3 times with 700 μl RNAiso reagent (Takara Bio Inc., Otsu, Shiga, Japan). For TECs, 700 μl RNAiso was added to the cell culture dishes, and the cell suspensions were collected and homogenized for 5 minutes at room temperature (RT). Next, 160 μl chloroform was added into the homogenized samples of kidneys and TECs. After that, the mixtures were shaken vigorously for 30 seconds, left to sit for 3 minutes at RT, and centrifuged 12,000 rpm for 15 minutes at 4℃. The aqueous phase, located in the top of the three phases, was carefully transferred to a fresh tube. The extracted RNA was precipitated with 400 μl isopropanol, and centrifuged at 12,000 rpm for 30 minutes at 4℃. RNA pellets were washed with 70% ethanol, air-dried for 2 minutes, and dissolved in sterile diethyl pyrocarbonate-treated distilled water. The quantity and quality of the extracted RNA were assessed by spectrophotometry at wavelengths of 260 and 280 nm.

6. Reverse transcription

연세대학교
YONSEI UNIVERSITY

A Takara cDNA synthesis kit (Takara Bio Inc., Otsu, Shiga, Japan) was used to obtain first-strand cDNA. Reverse transcription was carried out using 2 μg total RNA extracts with 10 μM random hexanucleotide primers, 1 mM dNTP, 8 mM $MgCl_2$, 30 mM KCl, 50 mM Tris-HCl at a pH of 8.5, 0.2 mM dithiothreithol, 25 U of RNase inhibitor, and 40 U of PrimeScript reverse transcriptase. The mixture was incubated for 10 minutes at 30℃ and for 1 hour at 42℃, then incubated for 5 minutes at 99℃ to deactivate the enzymes.

7. Quantitative real-time polymerase chain reaction

Reverse transcription of 1 μg total RNA was conducted using a cDNA kit (Takara Bio Inc., Otsu, Shiga, Japan). Then, quantitative real-time polymerase chain reaction (qPCR) was conducted in a total volume of 20 μl mixture, containing 10 μl SYBR Green PCR Master Mix (Applied Biosystems, Foster City, CA, USA). Primer concentrations were determined by preliminary experiments designed to identify their optimal concentrations of each primer. The qPCR conditions were as follows: 35 cycles of denaturation for 30 minutes at 94.5℃, annealing for 30 seconds at 60℃, and extension for 1 minute at 72℃. An initial heating was conducted for 9 minutes at 95℃ and a final extension was conducted for 7 minutes at 72℃ in all PCR reactions. The sequences of the primers used in this study are shown in Table 1. Each sample was run in triplicate in separated tubes, and a control without cDNA was included in each assay. After real-time PCR, the temperature was increased from 60 to 95℃ at a rate of 2℃/minute to construct a melting curve. cDNA data were normalized and analyzed using the comparative CT method ($2^{-\Delta\Delta CT}$). The results were determined as the relative expression normalized to that of 18s rRNA and are expressed in arbitrary units. Real-time PCR was conducted to compare

연세대학교
YONSEI UNIVERSITY

transcript levels of *Ppargc1a*, which is related to mitochondria biogenesis, energy metabolic regulator (*Ampk1*), mitochondrial transcripts (*Tfam* and *mtDNA*), mitochondrial dynamics (*Mfn* and *Drp1*), FAO (*Cpt1* and *Acox1*), glycolysis (*Hif1a, Glut1, Hk, Pkm2,* and *Ldha*), tricarboxylic acid (TCA) cycle (*Pdha, Sdha,* and *Fh*), fibrosis (*Fn1*, *Col1a1*, and *Acta2*) and apoptosis (*Bax* and *Bcl-2*), were assessed. All primers were obtained from Applied Biosystems.

Table 1. Primer sequences

Mouse Gene		Sequence (5'→ 3')
Ppargc1a	Forward	AGT CCC ATA CAC AAC CGC AG
	Reverse	CCC TTG GGG TCA TTT GGT GA
Ampk1	Forward	CTC AGT TCC TGG AGA AAG ATG G
	Reverse	CTG CCG GTT GAG TAT CTT CA
Tfam	Forward	GGA ATG TGG AGC GTG CTA AAA
	Reverse	TGC TGG AAA AAC ACT TCG GAA TA
mtDNA	Forward	TCC TCT GAC AGG ATT GCA GC
	Reverse	CCG AGG GTG AAT GAC CAG AG
Mfn	Forward	AAC GCT CTC TCT TTC GCA CG
	Reverse	TTG GAA AAC AGT GGG CTG GA
Drp1	Forward	GCT GCC TCA GAT CGT CGT AG
	Reverse	GGT GAC CAC ACC AGT TCC TC
Cpt1	Forward	GGT CTT CTC GGG TCG AAA GC
	Reverse	TCC TCC CAC CAG TCA CTC AC
Acox1	Forward	CTT GGA TGG TAG TCC GGA GA
	Reverse	TGG CTT CGA GTG AGG AAG TT
Hif1a	Forward	GG ATG AGT TCT GAA CGT CGA AA
	Reverse	AAT ATG GCC CGT GCA GTG AA
Glut1	Forward	ACA CTC ACC ACG CTT TGG TC
	Reverse	ACA CAC CGA TGA TGA AGC GG
Hk	Forward	CCA AAA TAG ACG AGG CCG TA
	Reverse	TTC AGC AGC TTG ACC ACA TC
Pkm2	Forward	TCGCATGCAGCACCTGATT
	Reverse	CCTCGAATAGCTGCAAGTGGTA
Ldha	Forward	GCT CCC CAG AAC AAG ATT ACA G
	Reverse	TCG CCC TTG AGT TTG TCT TC

연세대학교
YONSEI UNIVERSITY

Pdha	Forward	CTC CTG CCT CTG TGG TTG AG
	Reverse	ACA GCT GAA GTA GGT TCG CC
Sdha	Forward	CTC CTG CCT CTG TGG TTG AG
	Reverse	ACA GCT GAA GTA GGT TCG CC
Fh	Forward	GCA AGC CAA AAT TCC TTC CGT
	Reverse	CTC GCT TCA AGA TGC CGA AAG
Fn1	Forward	TGA CAA CTG CCG TAG ACC TGG
	Reverse	TAC TGG TTG TAG GTG TGG CCG
Col1a1	Forward	GCC AAG AAG ACA TCC CTG AA
	Reverse	GTT TCC ACG TCT CAC CAT TG
Acta2	Forward	CTG ACA GAG GCA CCA CTG AA
	Reverse	CAT CTC CAG AGT CCA GCA CA
Bax	Forward	TGC AGA GGA TGA TTG CTGAC
	Reverse	GAT CAG CTC GGG CAC TTT AG
Bcl-2	Forward	AGG AGC AGG TGC CTA CAA GA
	Reverse	GCA TTT TCC CAC CAC TGT CT
16s	Forward	ACC ATG AAG ACC ATG ACA CAG G
	Reverse	TGT CTT CCT TTT TAA GGC TGT CAA
18s	Forward	CGC TTC CTT ACC TGG TTG AT
	Reverse	GGC CGT GCG TAC TTA GAC AT

8. Western blot analysis

Using western blot analysis, I compared the expression levels of proteins related to mitochondria biogenesis, mitochondrial dynamics, the FAO pathway, fibrosis, and apoptosis. Harvested cultured cells and kidneys were lysed in sodium dodecyl sulfate (SDS) sample buffer composed of 2% SDS, 10 mM Tris-HCl with a pH of 6.8 and 10% (vol/vol) glycerol. Lysate was centrifuged at 10,000 × g for 10 minutes at 4℃, and the supernatant was stored at -70℃ until use. Protein concentrations were determined using a Bio-Rad kit (Bio-Rad Laboratories, Inc., Hercules, CA, USA). Laemmli sample buffer was added to 50 μg aliquots of the protein extracts, which then were heated for 5 minutes at 100℃ and electrophoresed in acrylamide denaturating SDS-polyacrylamide gel. The separated proteins were transferred to a Hybond-ECL membrane with a Hoeffer semidry

연세대학교
YONSEI UNIVERSITY

blotting apparatus (Hoeffer Instruments, San Francisco, CA, USA). After the protein was transferred to the membrane, it was incubated in blocking buffer A, which was composed of 1 × TBS, 0.1% Tween 20, and 5% nonfat milk for 30 minutes at RT, and then incubated overnight at 4℃ at a dilution of 1:1,000 with primary antibodies against the following proteins: peroxisome proliferator-activated receptor gamma coactivator 1-alpha (PGC-1α) (Abcam, Cambridge, MA, USA), phospho-AMP-activated protein kinase alpha 1 (pAMPK) (Cell Signaling Technology, MA, USA), carnitine palmitoyltransferase 1 (CPT1) (Novus Biologicals, Littleton, CO, USA), peroxisomal acyl-coenzyme A oxidase 1 (ACOX1) (Abcam, Cambridge, MA, USA), hypoxia-inducible factor 1-alpha (HIF-1α) (Novus Biologicals, Littleton, CO, USA), fibronectin (DAKO, Carpentaria, CA, USA), type I collagen (Southern Biotech, Birmingham, AL, USA), B-cell lymphoma 2 (BCL-2) (Santa Cruz Biotechnology, Santa Cruz, CA, USA), Bcl-2-associated X (BAX) (Santa Cruz Biotechnology, Santa Cruz, CA, USA), cleaved caspase 3 (Cell Signaling Technology, MA, USA), and β-actin (Sigma-Aldrich, St. Louis, MO, USA). Secondary antibodies were horseradish peroxidase-conjugated anti-goat, anti-rabbit, or anti-mouse IgG (all from Santa Cruz Biotechnology, Santa Cruz, CA, USA). After repeated washing, the membrane was developed using chemiluminescence reagent (ECL, Amersham Life Science, Loughborough, UK). ImageJ ver. 1.49 (National Institutes of Health, Bethesda, MD, USA; online at http://rsbweb.nih.gov/ij) was used to quantify band densities. Changes in the optical densities of the bands of the treated groups relative to control tissues and cells were analyzed.

9. Measurement of succinate, fumarate, and lactate concentrations

Concentrations of succinate, fumarate, and lactate were assessed colorimetrically

연세대학교
YONSEI UNIVERSITY

using commercially available assay kits (all from Abcam, Cambridge, MA, USA). Tissue and cell extractions were performed according to manufacturer instructions. Samples were loaded onto a 96-well plate and their absorbances at 450 nm were measured.

10. Measurement of oxygen consumption rates

An XF24 extracellular flux analyzer (Seahorse Bioscience, Billerica, MA, USA) was used to measure the rate of change of dissolved O_2 in the medium immediately surrounding adherent cells cultured in an XF24 V7 cell culture microplate. Mouse primary TECs cultured in DMEM supplemented with 1% FBS were seeded in an XF24 V7 cell culture microplate at 1.0×10^4 cells/well. Oxygen consumption rates, measured in pmol/minute, were assessed at baseline and after the addition of 2 μM ATP synthase inhibitor oligomycin and then 0.5 μM FCCP as an uncoupler. The final oxygen consumption rate was determined after adding 0.5 μM rotenone/antimycin A, an electron transport inhibitor.

11. Measurement of ATP levels

Total ATP concentrations were determined using an ATP colorimetric assay kit (Biovision, Mountain View, CA, USA). A total of 1×10^6 primarily cultured cells were lysed in 100 μl ATP assay buffer and centrifuged at 13,000 × g for 2 minutes at 4℃. Then 50 μl supernatants were added to 96-well plates and mixed with 50 μl reaction mix (ATP probe, ATP converter, developer mix in ATP assay buffer). The plates were incubated at RT for 30 minutes in the dark. The sample absorbance at 570 nm was determined using a microplate reader.

연세대학교
YONSEI UNIVERSITY

12. Transmission electron microscopy

Mitochondrial structures were examined by standard transmission electron microscopy. Kidney tissues and TECs were washed with precooled PBS at a pH of 7.4, postfixed in a mixture of 2% paraformaldehyde and 2.5% glutaraldehyde overnight, washed, dehydrated, and embedded in an epoxy resin following standard procedure. Ultrastructural images were captured with a JEOL 1011 microscope (JEOL, Tokyo, Japan).

13. Histological analysis and Masson's trichrome and immunofluorescence staining

To evaluate histological features, 10% formalin-fixed, paraffin-embedded kidney sections were stained with periodic acid–Schiff (PAS) and Masson's trichrome. PAS staining was done with dissolved paraffin on the tissue slides in an incubator at 60℃ for 30 minutes or more. Then the samples were sequentially rehydrated with xylene and 100%, 95%, and 90% alcohol. After washing the slides with distilled water and then soaking them in periodic acid for 7 minutes, the slides were reacted in Schiff's solution for 15 minutes. Modified Mayer's Hematoxylin counter-staining was performed after dehydration. Tubulointerstitial injury was scored semiquantitatively on PAS-stained tissues as described previously.[38] Tubulointerstitial injury was defined as tubular dilation, tubular atrophy, tubular cast formation, sloughing of tubular epithelial cells, or thickening of the tubular basement membrane and was scored on a scale ranging from 0 to 4. The scoring indicates which part of renal tissue was affected by tubulointerstitial injury: 0, no injury; 1, < 25%; 2, 25 to 50%; 3, 51 to 75%; 4, > 75%.

For Masson trichrome staining, 5-μm-thick sections of paraffin-embedded tissues were deparaffinized, rehydrated in ethyl alcohol, washed in tap water, and re-fixed in Bouin's solution for 1 hour at 56℃. After washing the samples in running tap water for

연세대학교
YONSEI UNIVERSITY

10 minutes and staining with Weigert iron hematoxylin working solution for 10 minutes, the slides were stained with Biebrich scarlet-acid fuchsin solution for 15 minutes and washed in tap water. The sections were differentiated in phosphomolybdic-phosphotungstic acid solution for 15 minutes, transferred to aniline blue solution, and stained for 10 minutes. After rinsing briefly in tap water, they were reacted with 1% acetic acid solution for 5 minutes. The intensity of Masson trichrome staining was scored on a scale of 1+ to 4+ compared with a negative control (score = 0), using a digital image analyzer (MetaMorph version 4.6r5; Universal Imaging, Los Angeles, CA, USA). The staining score was obtained based on the staining intensity score multiplied by the percentage of tubulointerstitium staining for that intensity.

For immunofluorescence staining of kidney samples, sections were deparaffinized, hydrated, and subject to microwave antigen retrieval in 10 mM sodium citrate with a pH of 6.0. Sections were blocked in 5% normal goat serum for 30 minutes at RT and incubated in anti–mouse COX IV antibody (Abcam, Cambridge, MA, USA) overnight at 4℃. Then, anti-mouse Alexa Fluor 488 (Cell Signaling Technology, Danvers, MA, USA) were applied. A semiquantitative staining intensity score was given after examining at least five fields in each section under x630 magnification using MetaMorph version 4.6r5 digital image analysis software (Universal Imaging, Los Angeles, CA, USA).

14. Statistical analysis

Statistical analysis was performed using SPSS 23.0 (IBM Corp., Chicago, IL, USA). Results were analyzed using a two-tailed Student *t* test or one-way ANOVA with post hoc

연세대학교
YONSEI UNIVERSITY

Tukey test. Differences with P values less than 0.05 were considered statistically significant.

III. RESULTS

1. *Lactobacillus acidophilus* KBL409 increases butyrate and acetate in the ceca of CKD mice

Figure 1 shows concentrations of two SCFAs, butyrate and acetate, in the ceca of CKD and KBL409-treated mice. The concentrations of butyrate and acetate in the ceca of adenine-induced CKD mice were significantly lower than those of the control group, but these were substantially restored by KBL409 administration. Notably, butyrate increased the transcript levels of *Ppargc1a*, a master regulator of mitochondrial biogenesis in renal TECs treated with TGF-β (Figure 2). Based on this finding, butyrate was used to explore the effects of SCFA on mitochondria in kidney TECs. Butyrate increased *Ppargc1a* levels in a dose dependent manner and *Ppargc1a* levels were highest at a dose of 10 mM, so I used 10 mM of butyrate in all *in vitro* analyses.

연세대학교
YONSEI UNIVERSITY

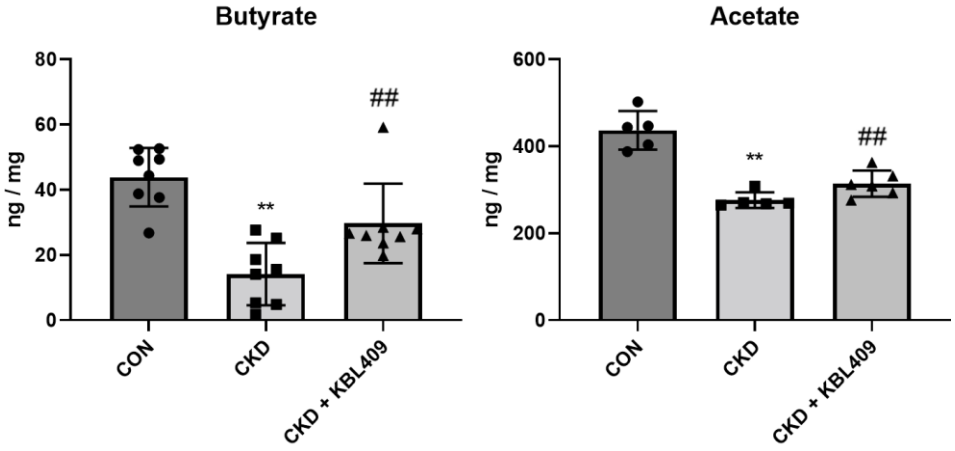

Figure 1. ***Lactobacillus acidophilus*** **KBL409 increases butyrate and acetate in the ceca of CKD mice.** SCFA levels in feces of adenine-induced CKD and KBL409-treated mice. Fecal butyrate and acetate levels were decreased in adenine-fed mice and restored by KBL409 administration. For all groups, data are means ± SEM (n = 5-8 per group).
**, P<0.05 vs. Con; ##, P<0.05 vs. CKD.

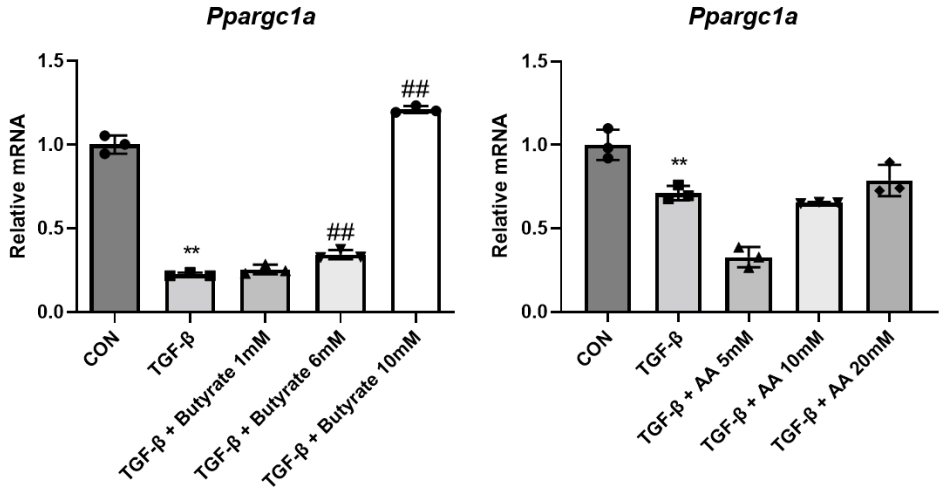

Figure 2. Butyrate increases the levels of *Ppargc1a* in a dose dependent manner. Treatment with 10 mM butyrate resulted in the highest mRNA expression levels of *Ppargc1a* in primary TECs treated with 10 ng/ml TGF-β. For all groups, data are means ± SEM (n = 3 per group).
**, P<0.05 vs. Con; ##, P<0.05 vs. TGF-β.

연세대학교
YONSEI UNIVERSITY

2. KBL409 supplementation improves mitochondrial biogenesis, dynamics, and morphology in CKD mice

First, I examined the effects of KBL409 administration on expression levels of *Ppargc1a* and *Ampk1*, key regulators of energy metabolism. In adenine-fed with CKD mice, the transcript and protein expression levels of these two regulators were significantly lower than those in control mice. The decreases in these regulator levels were significantly increased by KBL409 administration (Figure 3A and 3B). I then examined mitochondrial dynamics-related genes and morphology. The mRNA expression levels of mitofusin (*Mfn*), a mitochondrial fusion-related gene, were significantly decreased in CKD mice compared with control mice, whereas those of dynamin-related protein 1 (*Drp1*), a mitochondrial fission-related gene, were increased. These alterations were restored by KBL409 (Figure 3C). Electron microscopy confirmed that cristae were disrupted, and mitochondria were fragmented in the kidney TECs of adenine-fed mice and that these abnormalities were significantly attenuated by KBL409 supplementation (Figure 3D). In addition, KBL409 restored the decreased expression of mitochondrial transcripts, such as *Tfam* and *mtDNA*, in adenine-fed mice (Figure 3E). Thus, KBL409 improved mitochondrial biogenesis, dynamics, and morphology in mice with adenine-induced CKD.

연세대학교
YONSEI UNIVERSITY

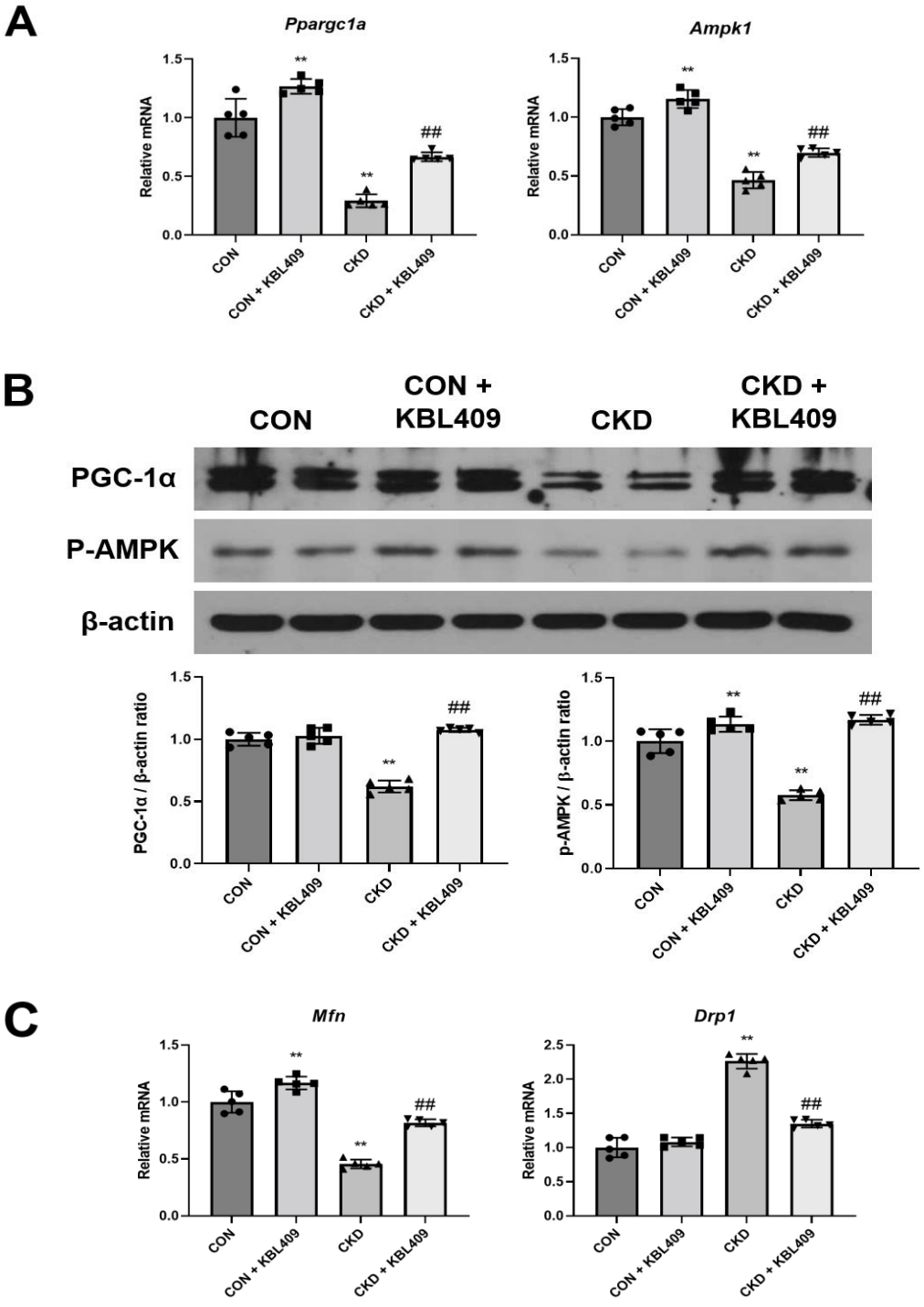

연세대학교
YONSEI UNIVERSITY

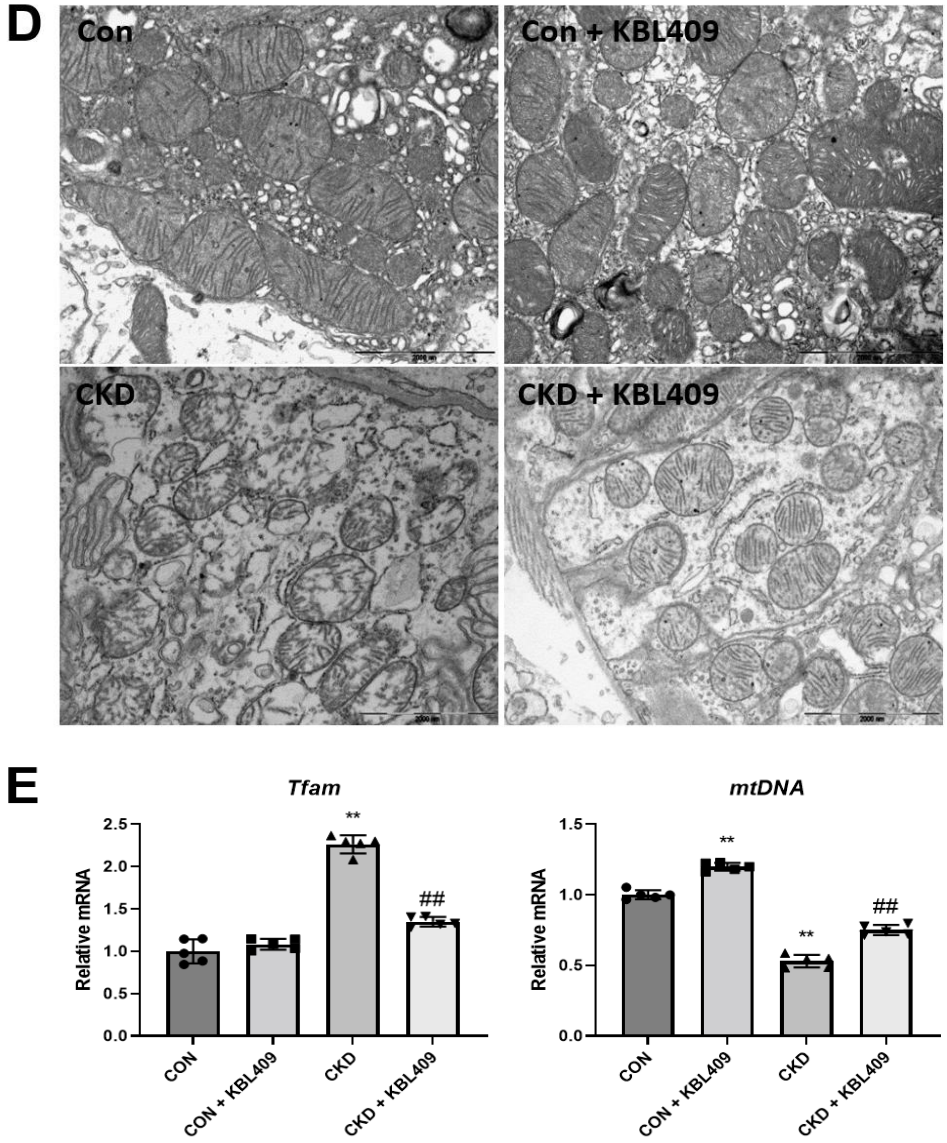

Figure 3. KBL409 supplementation improves mitochondrial biogenesis, dynamics, and morphology in CKD mice. (A) The mRNA expression levels of *Ppargc1a* and *Ampk1* and (B) the corresponding protein levels of PGC-1α and phospho-AMPK were reduced in adenine-induced CKD, which were restored by KBL409 supplementation. (C) The mRNA transcript analysis of *Mfn* and *Drp1*, and (D) electron microscopic images of kidney mitochondria in CKD mice showed a shift in mitochondrial dynamics toward fission and disrupted mitochondrial integrity. These alterations were attenuated by KBL409 administration. (E) The decreased mRNA expression levels of mitochondrial transcripts in CKD mice were restored by supplementation with KBL409.

연세대학교
YONSEI UNIVERSITY

For all groups, data are means ± SEM (n = 5 per group).
**, P<0.05 vs. Con; ##, P<0.05 vs. CKD.

In vitro, treatment with TGF-β and PCS in TECs recapitulated the findings of the animal study (Figures 4 and 5). Butyrate administration restored the decreased immunofluorescence intensity in TECs stimulated with TGF-β and PCS (Figure 5C).

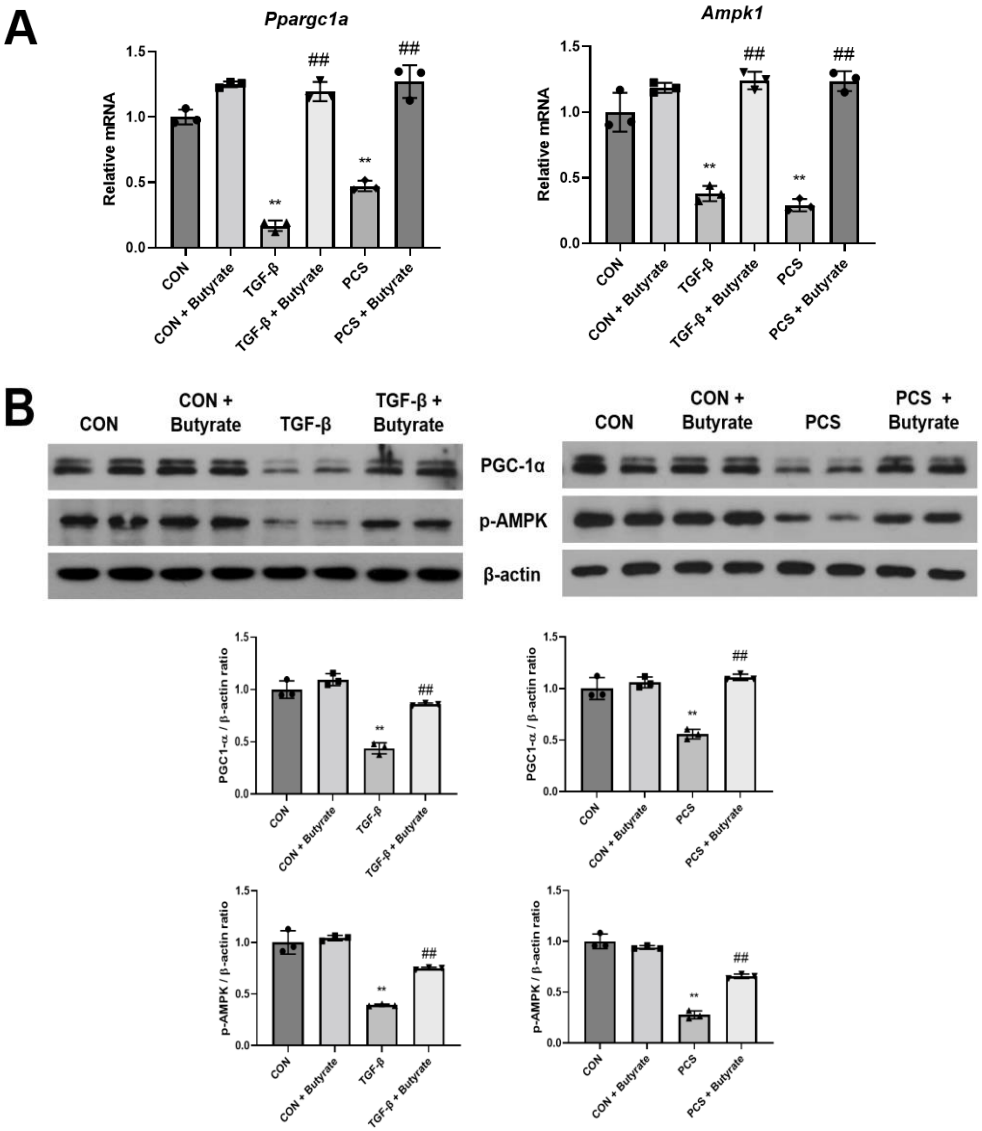

연세대학교
YONSEI UNIVERSITY

Figure 4. Butyrate increases the expression of key regulators of mitochondrial biogenesis in TECs exposed to TGF-β and PCS. Primary TECs were stimulated with 10 ng/ml TGF-β and 0.5 mM PCS in the presence of 10 mM butyrate for 48 hr. (A) The mRNA expression levels of *Ppargc1a* and *Ampk1* and (B) the corresponding protein levels of PGC-1α and phospho-AMPK were decreased in TECs stimulated with TGF-β and PCS, which were restored by butyrate. For all groups, data are means ± SEM (n = 3 per group).
**, P<0.05 vs. Con; ##, P<0.05 vs. TGF-β and PCS.

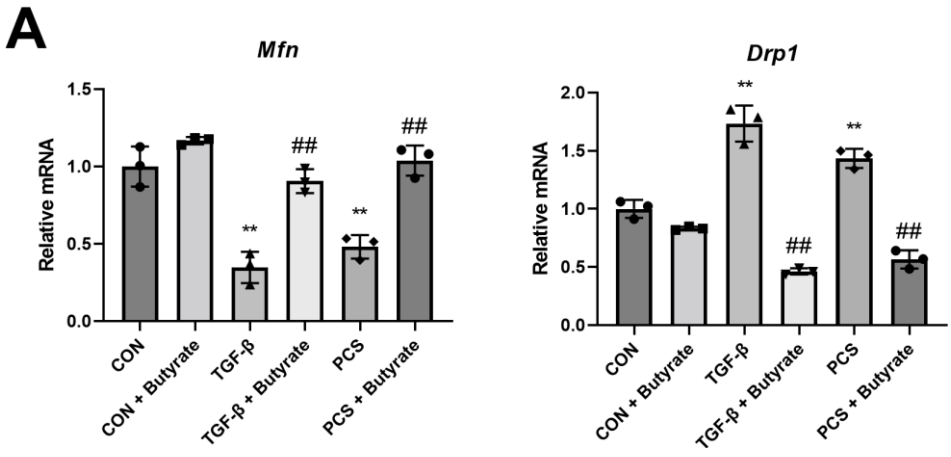

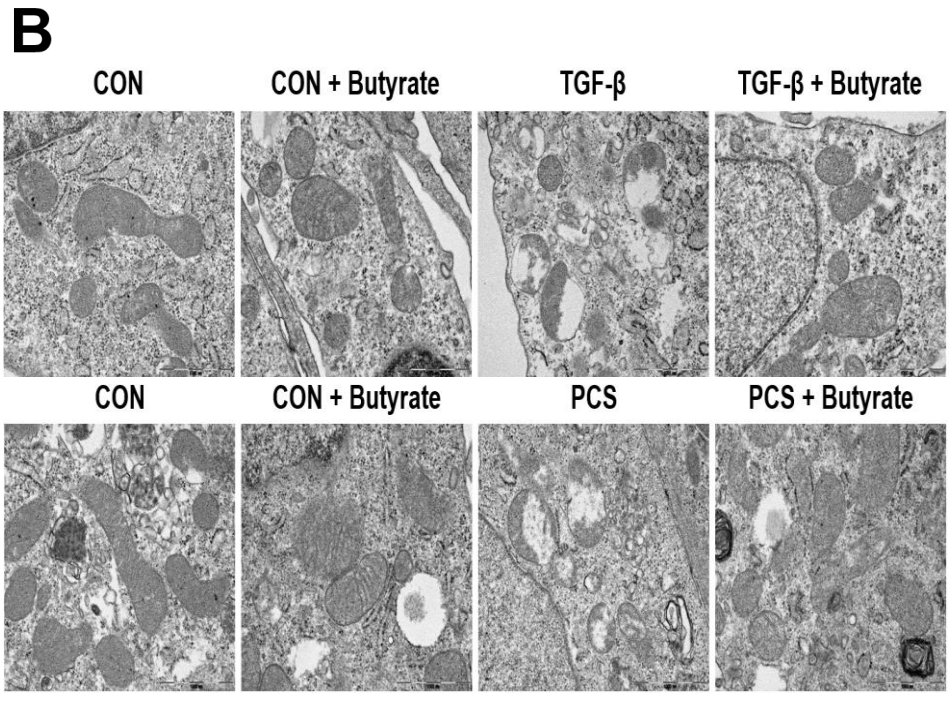

연세대학교
YONSEI UNIVERSITY

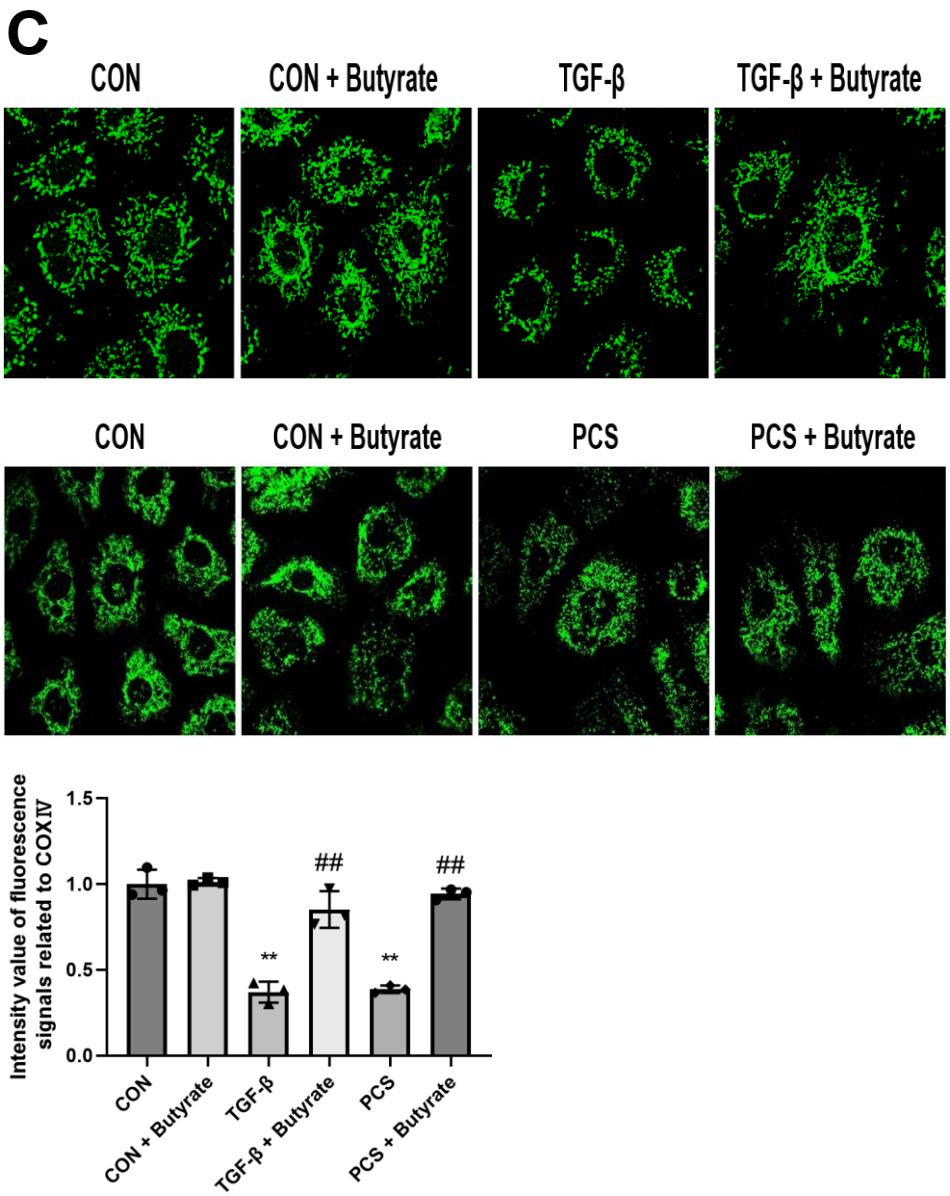

연세대학교
YONSEI UNIVERSITY

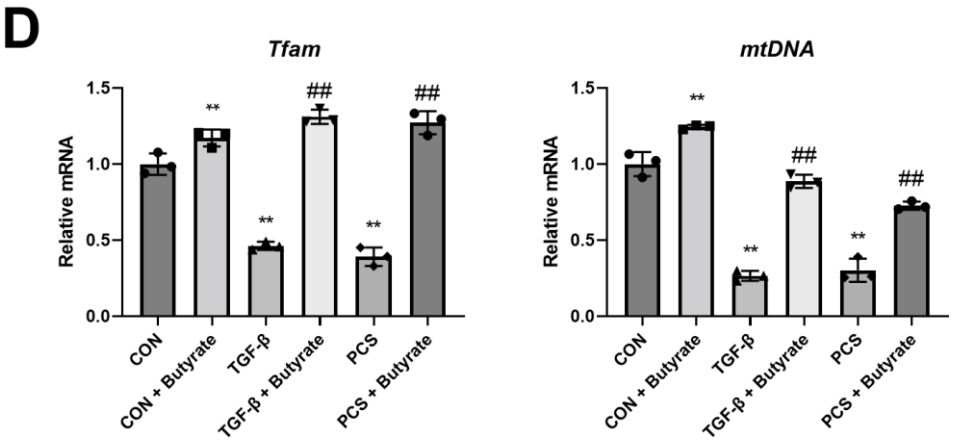

Figure 5. Butyrate improves mitochondrial dynamics and morphology in TECs exposed to TGF-β and PCS. Primary TECs were stimulated with 10 ng/ml TGF-β and 0.5 mM PCS in the presence of 10 mM butyrate for 48 hr. (A) In TECs stimulated with TGF-β and PCS, the mRNA expression levels of *Mfn* were decreased, while those of *Drp1* were increased compared with control. These alterations were reversed by butyrate treatment. (B) Representative sections of mitochondria in TECs using electron microscopy and (C) immunofluorescence staining for COX IV. TECs pretreated with TGF-β and PCS exhibited increased fragmented cristae in the sections, which were attenuated by butyrate. (D) The decreased mRNA expression levels of mitochondrial transcripts in TECs treated with TGF-β and PCS were restored by butyrate. For all groups, data are means ± SEM (n = 3 per group).
**, P<0.05 vs. Con; ##, P<0.05 vs. TGF-β and PCS.

3. KBL409 attenuates the altered mitochondrial metabolism in CKD mice

PGC-1α and AMPK are metabolic regulators and their expression levels were decreased in CKD mice compared with control mice, so I examined the expression levels of the key enzymes for FAO, glycolysis, and the TCA cycle. First, I observed that the transcript and protein levels of two rate-limiting enzymes of FAO, *Cpt1* and *Acox1,* were markedly lower in CKD mice. Theses alterations were significantly resorted by KBL409 supplementation (Figure 6A and 6B). In addition, I also quantified the transcript levels of key genes related to the glycolytic pathway, such as *Hif1a, Glut1, Hk, Pkm2,* and *Ldha.* The mRNA expression levels of *Hif1a* were significantly increased in CKD mice

연세대학교
YONSEI UNIVERSITY

compared with control mice, while those of *Glut1*, *Hk*, *Pkm2*, and *Ldha* were decreased (Figure 7A). Accordingly, more L-lactate was produced in CKD mice (Figure 7B). Furthermore, the expression levels of genes involved in the TCA cycle including *Pdha*, *Sdha*, and *Fh*, were significantly lower in CKD mice than in controls (Figure 7A). These reduced gene expression levels led to the accumulation of fumarate and succinate, the TCA cycle intermediates, indicating that the TCA cycle was impaired (Figure 7B). All these changes were reversed by KBL409 supplementation. Taken together, KBL409 improved the altered mitochondrial metabolism in CKD mice.

연세대학교
YONSEI UNIVERSITY

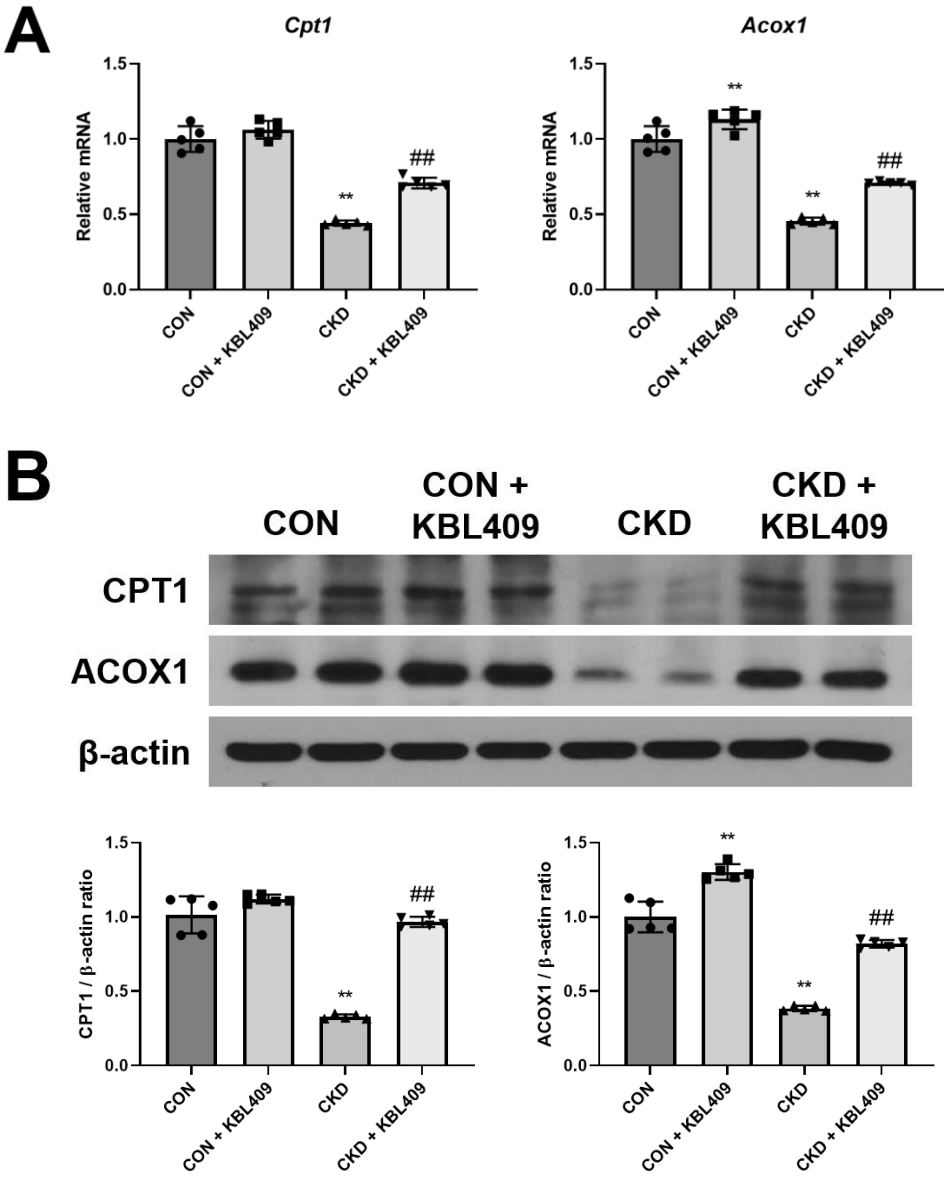

Figure 6. KBL409 improves the suppressed mitochondrial fatty acid oxidation in CKD mice. (A) The mRNA and (B) protein expression levels of CPT1 and ACOX1, markers for fatty acid oxidation were reduced in CKD mice and these were increased by KBL409 supplementation. For all groups, data are means ± SEM (n = 5 per group).
**, P<0.05 vs. Con; ##, P<0.05 vs. CKD.

연세대학교
YONSEI UNIVERSITY

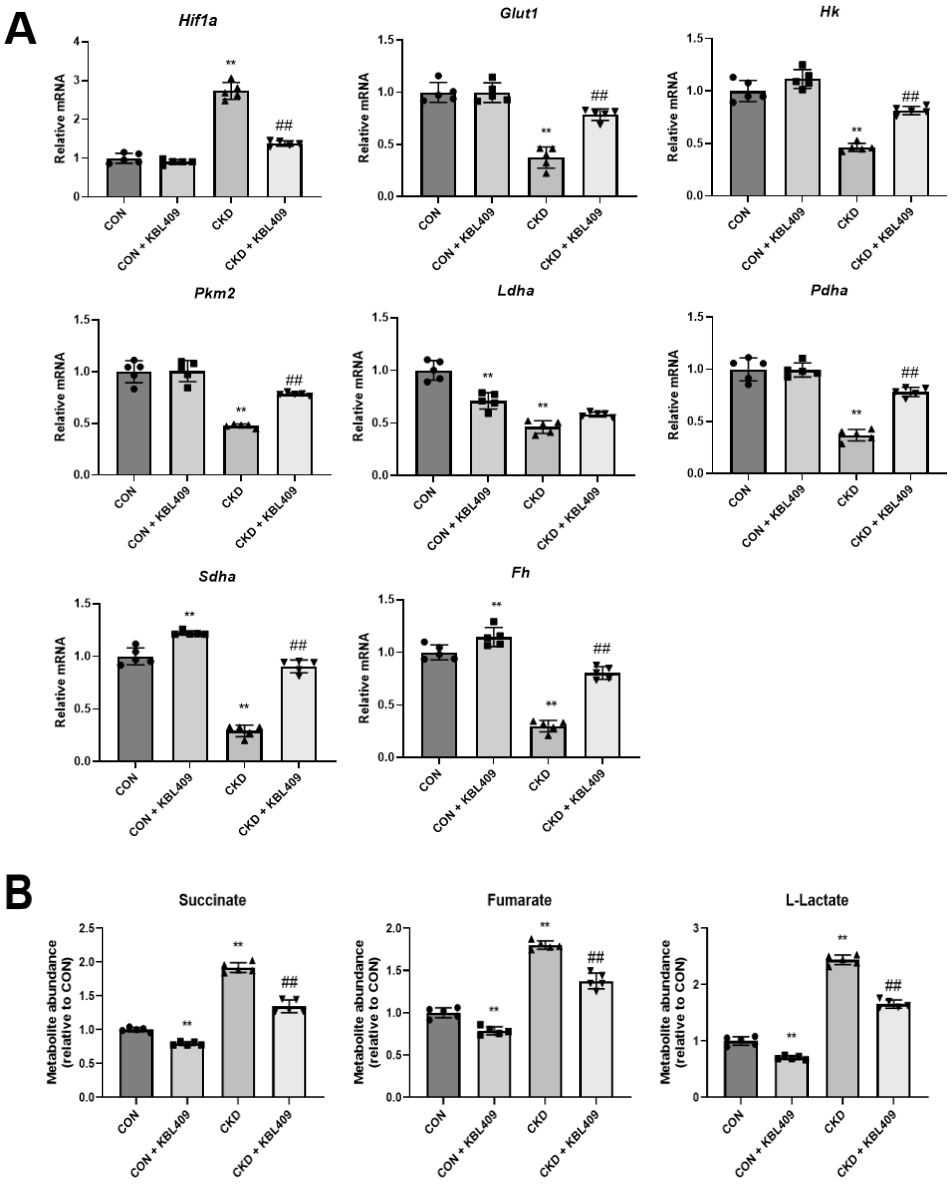

Figure 7. KBL409 restores the altered mitochondrial glucose oxidation and TCA cycle in CKD mice. (A) Glucose oxidation and TCA cycle were dysregulated as evidenced by the altered transcript levels of genes involved in these pathways and (B) the concentrations of the TCA cycle intermediates were increased in adenine-fed mice. All these alterations were reversed by KBL409 administration. For all groups, data are means ± SEM (n = 5 per group).
**, P<0.05 vs. Con; ##, P<0.05 vs. CKD.

연세대학교
YONSEI UNIVERSITY

In line with the results of metabolic assay in the animal study, treatment with SCFAs rescued the suppressed metabolic pathway including FAO, glycolysis, and the TCA cycle in TECs treated with TGF-β and PCS (Figure 8 and 9).

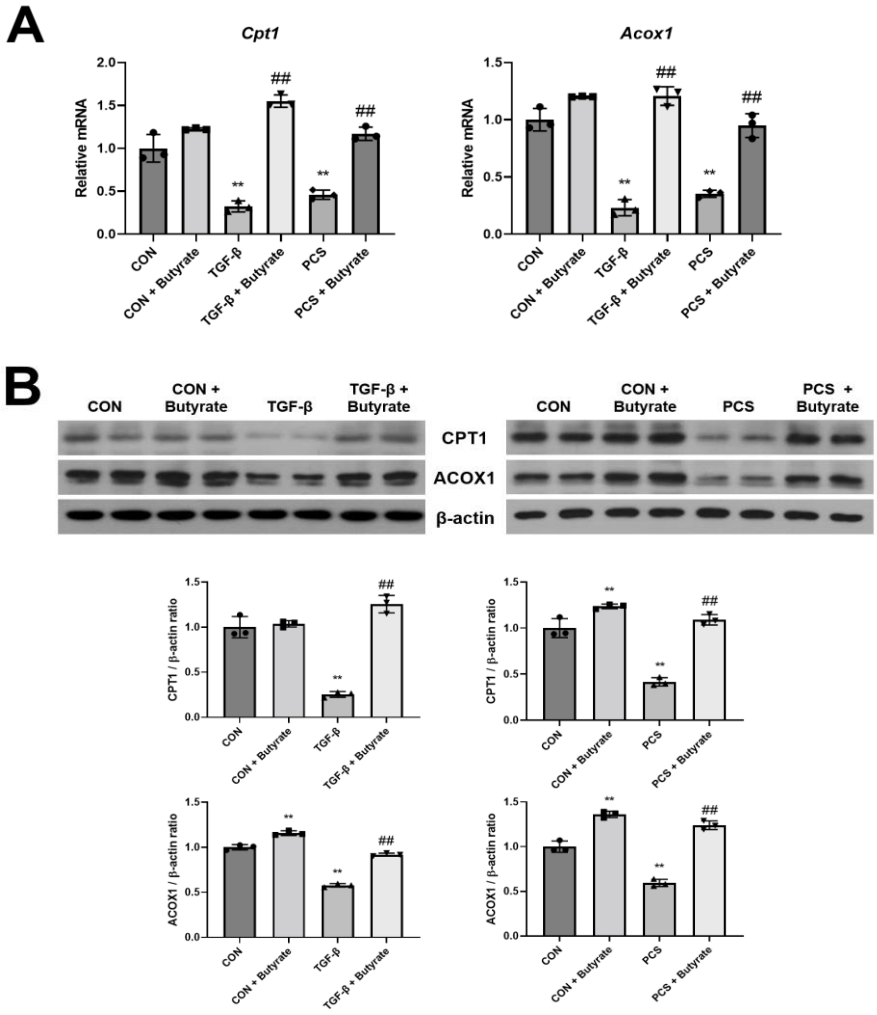

Figure 8. Butyrate improves the suppressed mitochondrial fatty acid oxidation in TECs exposed to TGF-β and PCS. Primary TECs were stimulated with 10 ng/ml TGF-β and 0.5 mM PCS in the presence of 10mM butyrate for 48 hours. (A) The mRNA and (B) protein expression levels of markers for fatty acid oxidation were decreased in TECs treated with TGF-β and PCS, which were reversed by butyrate administration. For all groups, data are means ± SEM (n = 3 per group).
**, P<0.05 vs. Con; ##, P<0.05 vs. CKD.

연세대학교
YONSEI UNIVERSITY

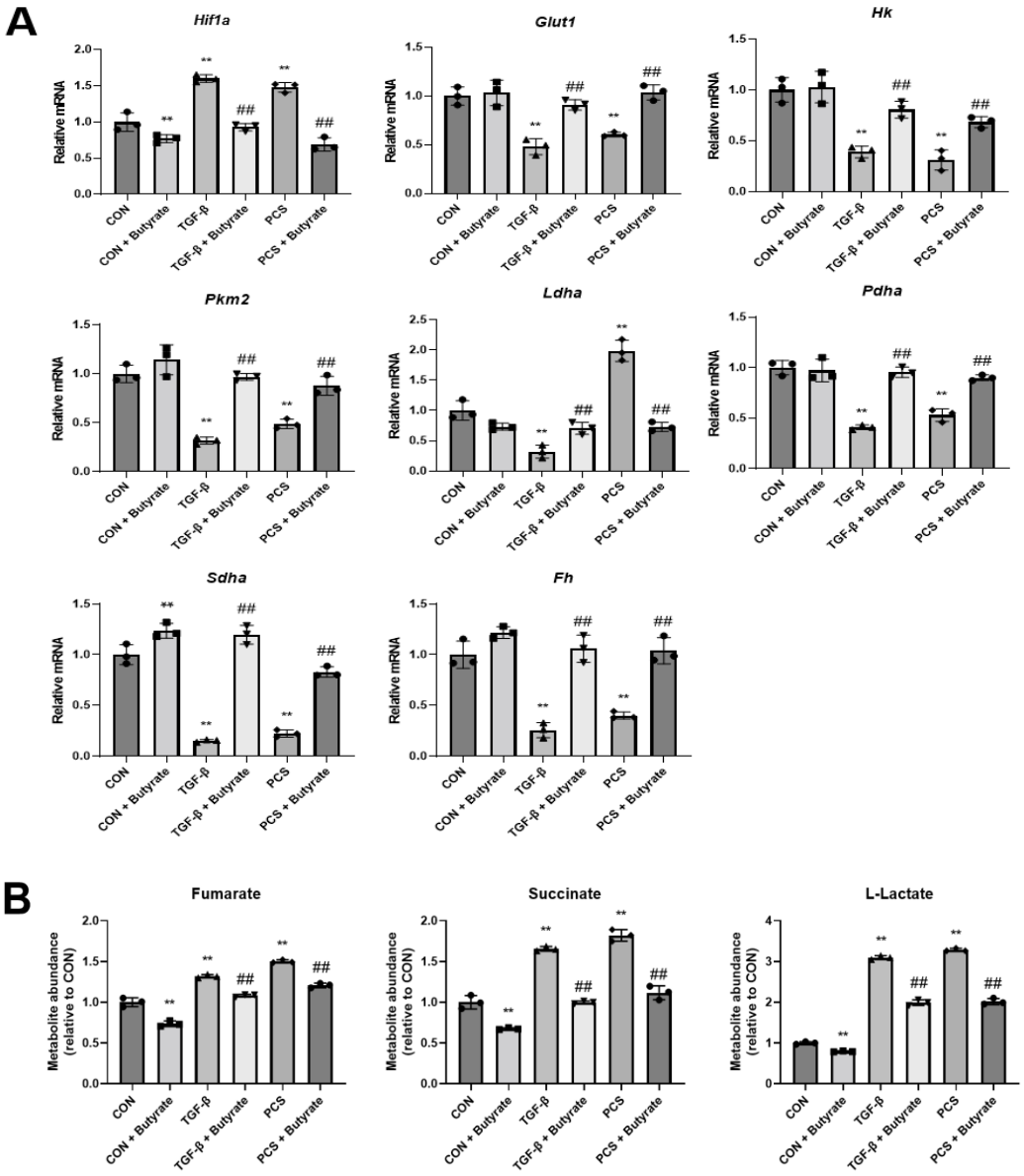

Figure 9. Butyrate restores the mitochondrial glucose oxidation and the TCA cycle in TECs exposed to TGF-β and PCS. Primary TECs were stimulated with 10 ng/ml TGF-β and 0.5 mM PCS in the presence of 10mM butyrate for 48 hours. (A) Glucose oxidation and the TCA cycle were dysregulated as evidenced by the altered transcript levels of genes involved in these pathways and (B) the concentrations of the TCA cycle intermediates were increased in TECs treated with TGF-β and PCS. All these changes were restored by butyrate administration. For all groups, data are means ± SEM (n = 3 per group).
**, P<0.05 vs. Con; ##, P<0.05 vs. TGF-β and PCS.

연세대학교
YONSEI UNIVERSITY

4. Mitochondrial respiration and ATP production are improved by KBL409 supplementation

I confirmed significant defects in mitochondrial metabolism in adenine-fed mice by mitochondrial function assay using a Seahorse analyzer. Oxidative phosphorylation was lower in CKD mice than in control mice as evidenced by decreases in basal respiration, ATP production, maximal respiration, and spare respiratory capacity in kidney TECs derived from adenine-induced CKD mice. KBL409 supplementation improved these alterations, indicating that mitochondrial respiration was restored (Figure 10A). The decreased energy utilization in CKD mice reduced ATP levels as determined by an ATP colorimetric assay kit. KBL409 supplementation recovered ATP levels (Figure 10B). These findings were also confirmed by *in vitro* analysis (Figure 11). In aggregates, KBL409 restored impaired mitochondrial respiration and energy metabolism, and decreased ATP production in CKD mice.

연세대학교
YONSEI UNIVERSITY

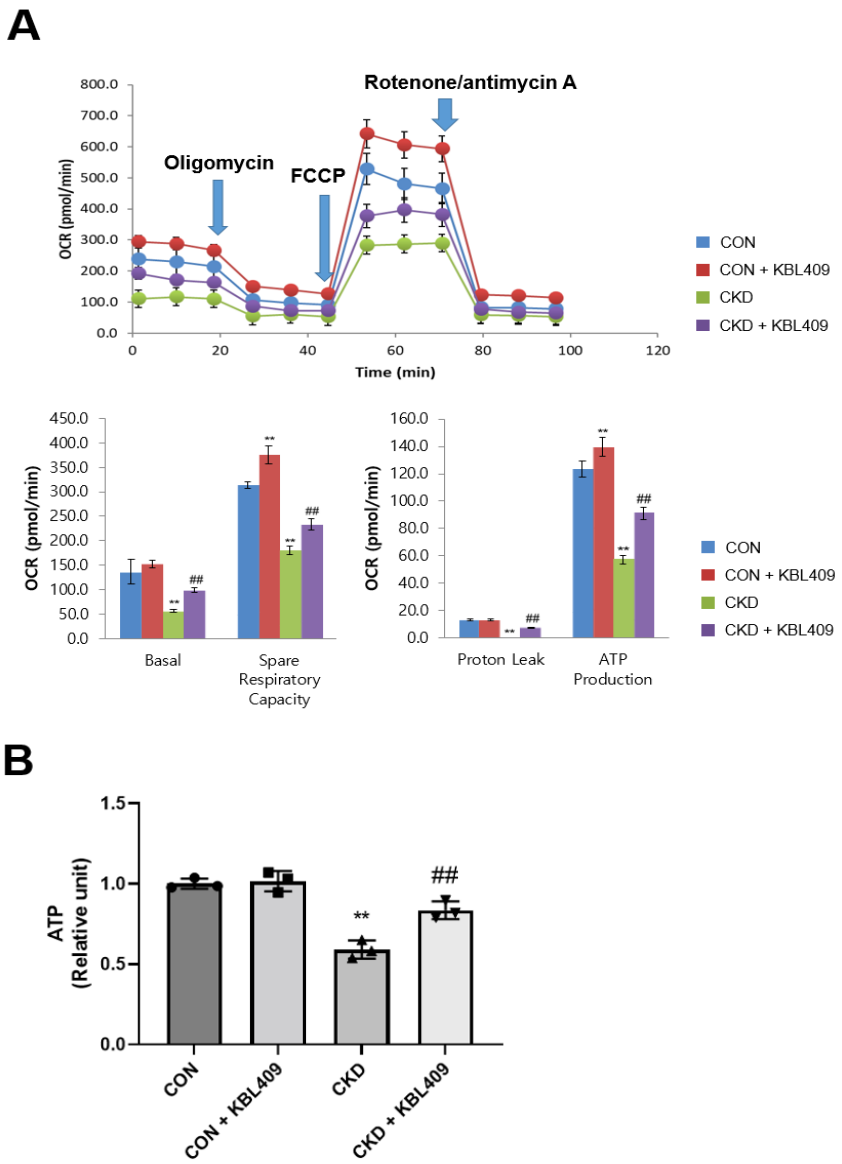

Figure 10. Mitochondrial respiration and ATP production after KBL409 supplementation. (A) Oxygen consumption rates (OCRs) in kidney TECs of CKD mice. 2 μM oligomycin, 0.5 μM FCCP and 0.5 μM rotenone/antimycin A were injected sequentially at the time points indicated. Adenine-induced CKD mice exhibited significant reductions in basal OCRs, spare respiratory capacity, proton leak, and ATP production. These alterations were reversed by KBL409 administration. (B) KBL409 supplementation in CKD mice significantly increased the ATP levels. For all groups, data are means ± SEM (n = 3 per group).
**, P<0.05 vs. Con; ##, P<0.05 vs. CKD.

연세대학교
YONSEI UNIVERSITY

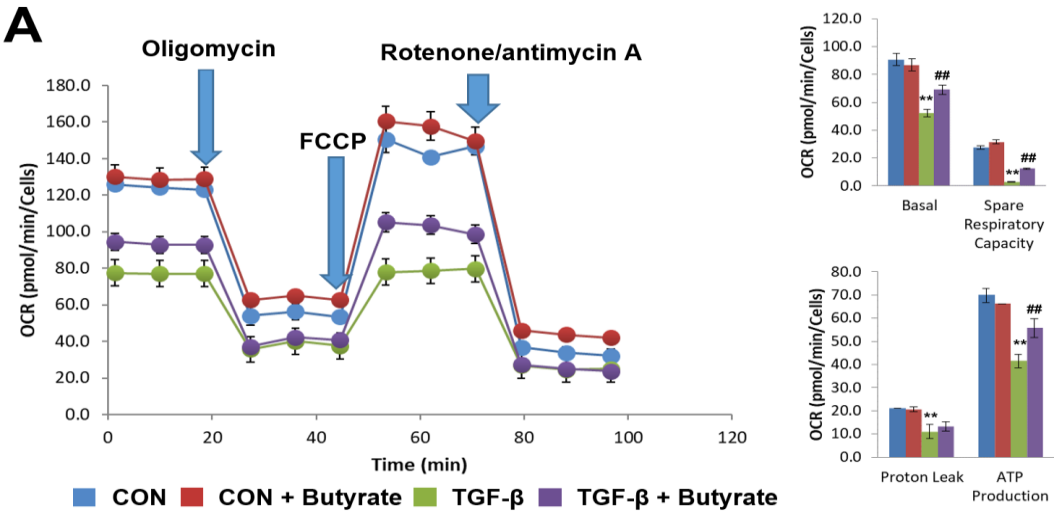

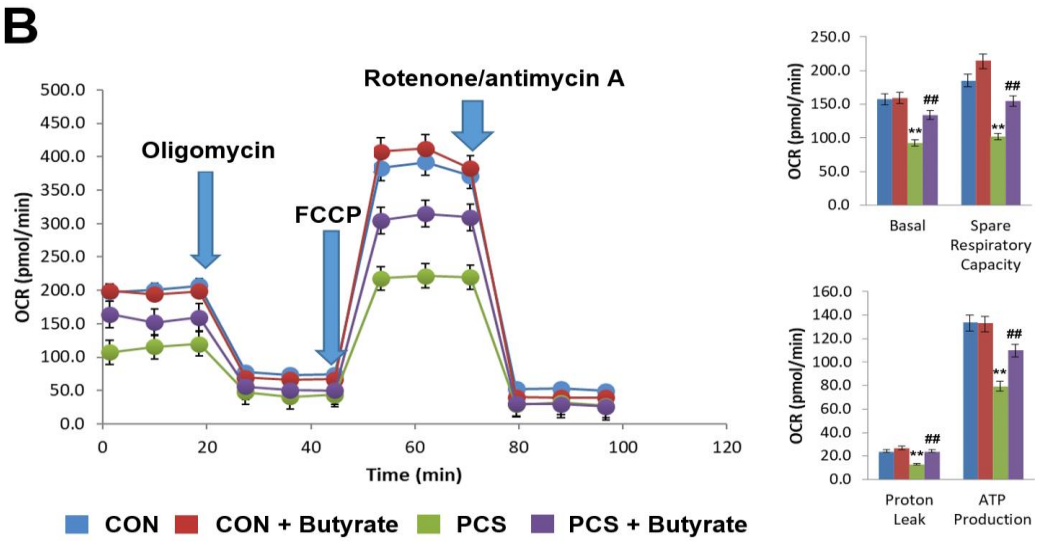

연세대학교
YONSEI UNIVERSITY

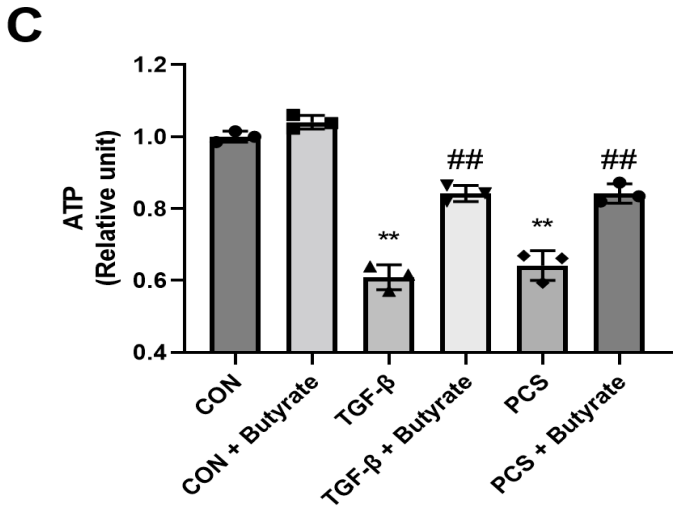

Figure 11. Mitochondrial dysfunction in TECs exposed to TGF-β and PCS is improved by butyrate supplementation. Primary TECs were stimulated with 10 ng/ml TGF-β and 0.5 mM PCS in the presence of 10mM butyrate for 48 hours. (A) Oxygen consumption rates (OCRs) in kidney TECs. 2 μM oligomycin, 0.5 μM FCCP and 0.5 μM rotenone/antimycin A were injected sequentially at the time points indicated. TECs exposed to (A) TGF-β and (B) PCS showed significant reductions in basal OCRs, spare respiratory capacity, proton leak, and ATP production. All these changes were restored by butyrate. (C) Treatment with butyrate significantly increased the ATP levels in TECs treated with TGF-β and PCS. For all groups, data are means ± SEM (n = 3 per group).
**, P<0.05 vs. Con; ##, P<0.05 vs. TGF-β and PCS.

5. KBL409 alleviates renal fibrosis and apoptosis in CKD mice

Renal histopathology was examined by PAS and Masson's trichrome staining. In adenine-fed CKD mice, severe tubular degeneration, widening of the interstitium, and severe interstitial fibrosis were observed (Figure 12A). However, treatment with KBL409 alleviated this fibrotic change. Masson's trichrome staining corroborated this finding. Interstitial collagen accumulation and fibrotic lesion were ameliorated by KBL409 supplementation (Figure 12B).

연세대학교
YONSEI UNIVERSITY

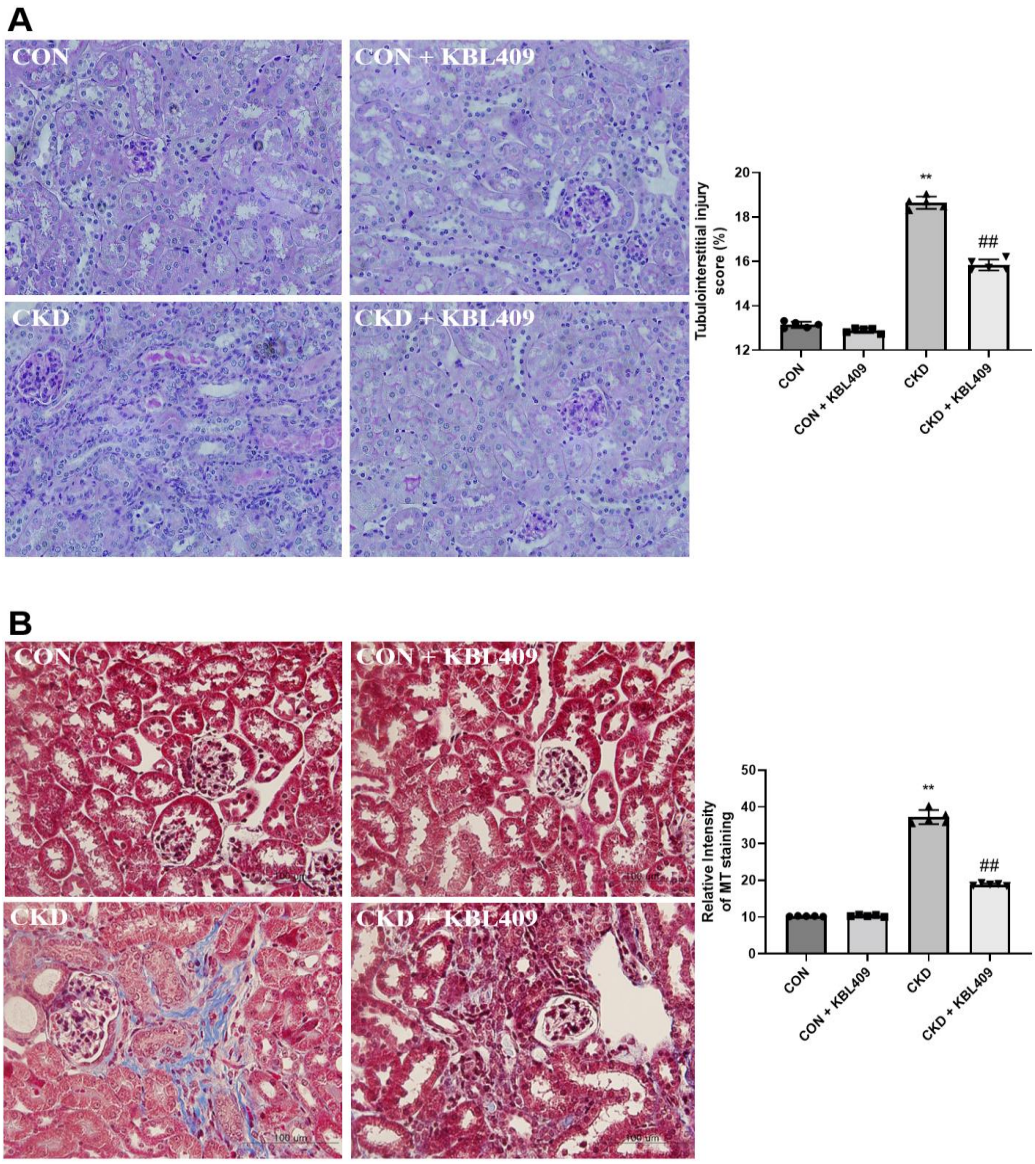

Figure 12. Kidney injury and fibrotic area are diminished by KBL409 supplementation.
Histological examinations by (A) PAS and (B) Masson's trichrome staining showed the attenuated fibrotic changes in adenine-induced mice with KBL409 supplementation. For all groups, data are means ± SEM (n = 5 per group).
**, P<0.05 vs. Con; ##, P<0.05 vs. CKD.

연세대학교
YONSEI UNIVERSITY

These structural alterations were concomitant with changes in the expression levels of profibrotic genes including *Fn1, Col1a1, and Acta2* (Figure 13A and B). KBL409 supplementation also significantly reduced the increased expression of Bax/Bcl-2 and cleaved-caspase 3 in CKD mice, indicating attenuated apoptotic cell death. Thus, KBL409 supplementation in CKD mice improved kidney fibrosis and reduced apoptosis.

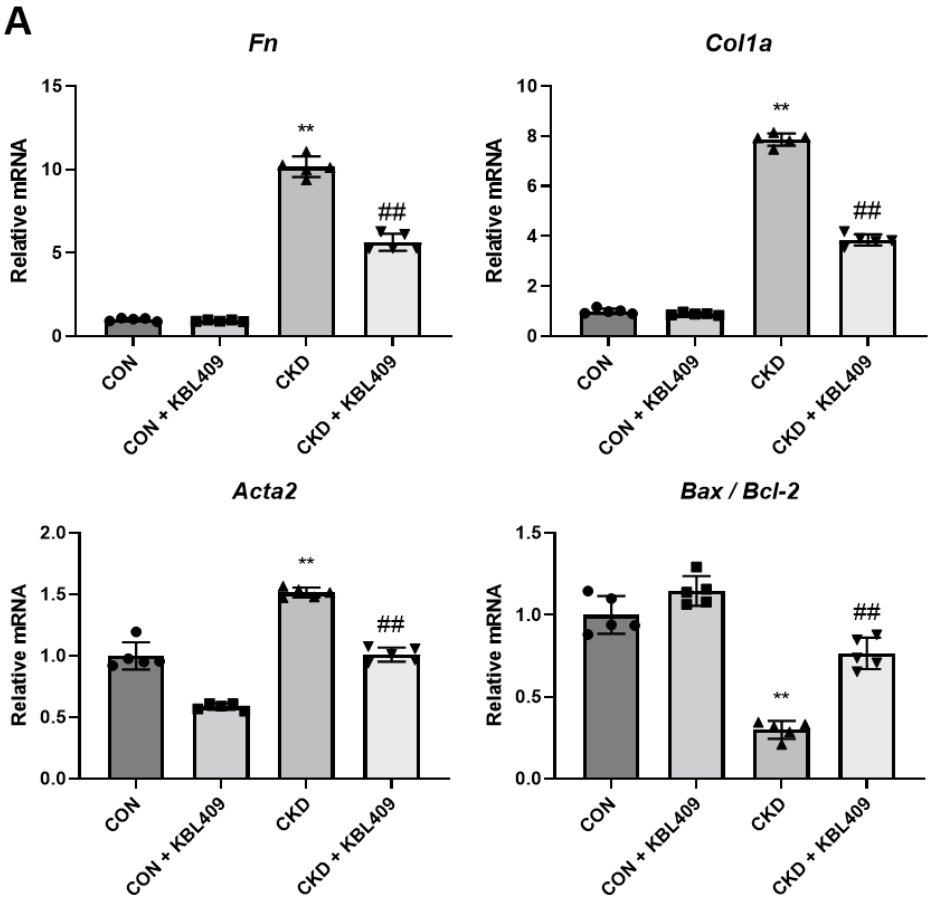

연세대학교
YONSEI UNIVERSITY

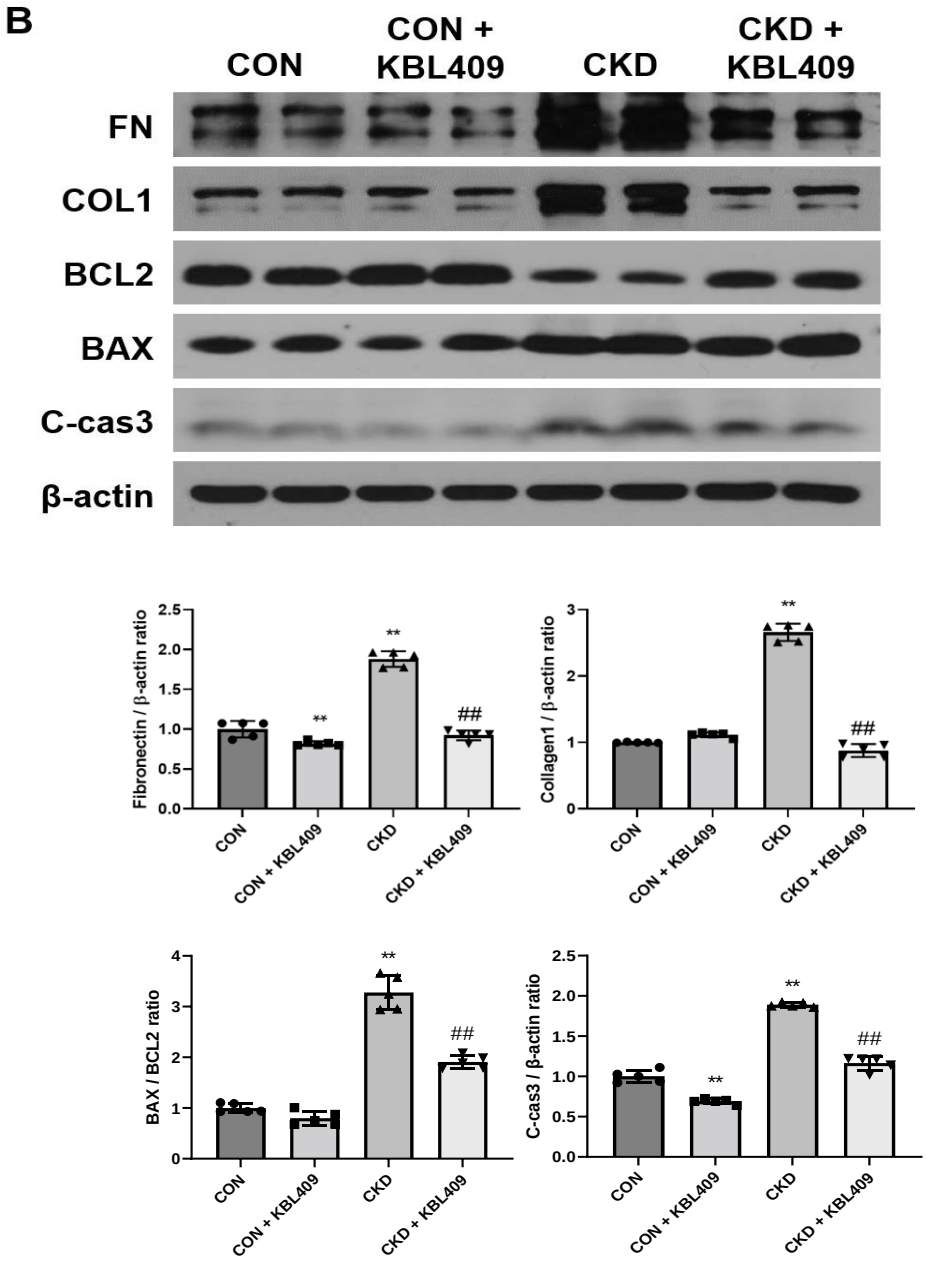

Figure 13. KBL409 reduces the expression of profibrotic and apoptotic markers in CKD mice. (A) The mRNA and (B) protein expressions of pro-fibrotic markers and apoptotic cell death markers were attenuated in CKD mice with KBL409 supplementation. For all groups, data are means ± SEM (n = 5 per group).
**, P<0.05 vs. Con; ##, P<0.05 vs. CKD.

연세대학교
YONSEI UNIVERSITY

Accordingly, SCFAs treatment decreased the increased expression levels of profibrotic markers and apoptotic cell death in TECs incubated with TGF-β and PCS (Figure 14).

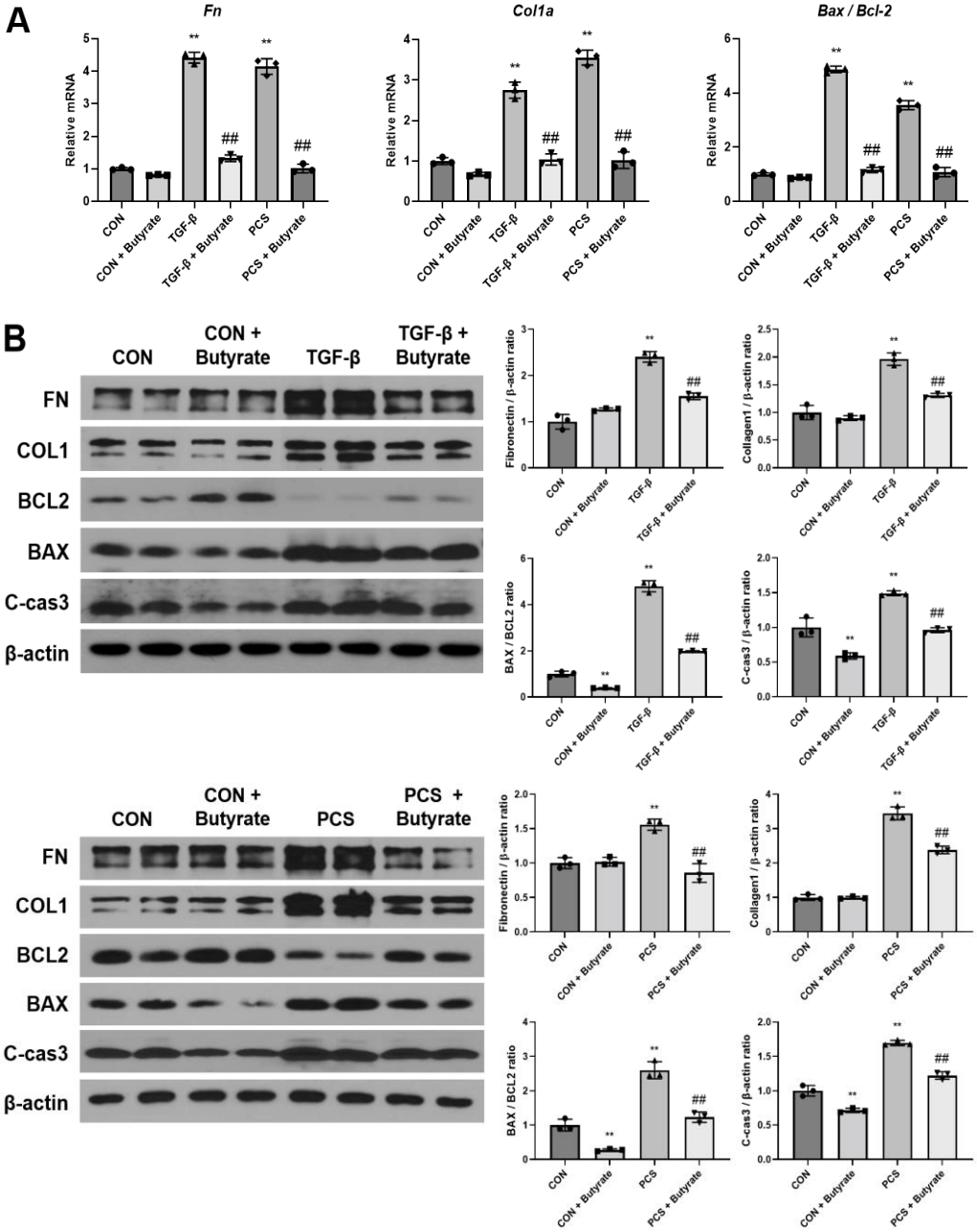

연세대학교
YONSEI UNIVERSITY

Figure 14. Butyrate reduces the expression of profibrotic and apoptotic markers in TECs exposed to TGF-β and PCS. Primary TECs were stimulated with 10 ng/ml TGF-β and 0.5 mM PCS in the presence of 10 mM butyrate for 48 hours. (A) The mRNA and (B) protein expressions of pro-fibrotic markers and apoptotic cell death markers were increased in TGF-β and PCS-stimulated TECs, which were attenuated by butyrate administration. For all groups, data are means ± SEM (n = 3 per group).
**, P<0.05 vs. Con; ##, P<0.05 vs. TGF-β and PCS.

IV. DISCUSSION

In this study, I demonstrated that *Lactobacillus acidophilus* KBL409 improved the impaired mitochondrial biogenesis and dysregulated mitochondrial dynamics in a murine model of adenine-induced CKD. These effects improved energy metabolism and mitochondrial function, ultimately resulting in decreased cell death and fibrosis. A schematic figure summarizing the mechanisms by which KBL409 supplementation has this effect in light of preserving mitochondrial function is presented in Figure 15.

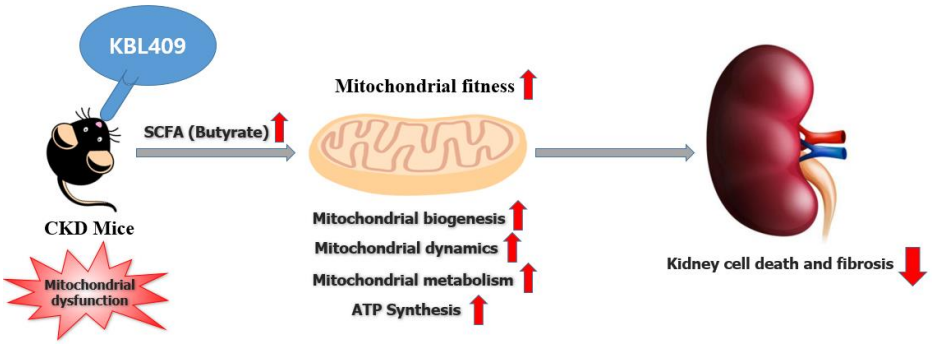

Figure 15. A schematic summary of the molecular mechanisms by which KBL409 protects against kidney injury via preserving mitochondrial function.

Uremia profoundly alters the composition of the microbial flora.[39] Increased influx of uremic toxins and CKD-associated dietary and pharmacologic intervention can lead to intestinal dysbiosis and excessive growth of pathobionts.[21] Dysbiosis contributes to

연세대학교
YONSEI UNIVERSITY

intestinal barrier dysfunction by the disintegration of colonic epithelial tight junctions.[40] Increased intestinal permeability leads to the translocation of uremic toxins and bacteria, which triggers systemic inflammation and progressive fibrosis in CKD.[21,24,41] Dysbiosis also results in increased production of bacteria-derived uremic toxins, amplifying the loop of uremic solute accumulation.[22] Thus, targeting gut microbiota might be a useful therapeutic strategy for delaying the progression of CKD. Prebiotic and probiotic supplementation have been shown to reduce uremic toxins and inflammation and can restore kidney function.[23-27] However, clinical trials in human have shown mixed results.[42-48] Therefore, many studies are being conducted to find the optimal species for treating specific clinical diseases. Of note, my coworkers previously demonstrated that supplementation with *Lactobacillus acidophilus* KBL409 in an animal model of CKD preserved kidney function and reduced albuminuria by maintaining the integrity of the intestinal barrier, reducing inflammation and oxidative stress via immunomodulation.[36] In the present study, I further showed that KBL409 protects against kidney injury by improving mitochondrial biogenesis and energy metabolism.

Mitochondrial biogenesis is a finely tuned process requiring the coordinated expression of genes in the nucleus and mitochondria. PGC-1α is a master regulator of mitochondrial biogenesis and energy metabolism that allows for a more concerted control of interconnected transcription factors.[49] PGC-1α activity is low in CKD and restoring it protects against kidney injury.[50-55] For instance, PGC-1α was downregulated in different murine kidney disease models including folic acid-induced kidney fibrosis and Notch transgenic mice, whereas the tubule-specific overexpression of PGC-1α reduced fibrosis in both models.[53,54] In keeping with these findings, my study demonstrated that KBL409 administration restored the expression of key metabolic regulators such as PGC-1α and

연세대학교
YONSEI UNIVERSITY

AMPK; improved mitochondrial energy metabolism and morphological structure; and mitigated mitochondrial dysfunction, all of which in turn decreased cell death and fibrosis in CKD model. This improvement in CKD phenotype could be attributed to the increased FAO and glycolysis induced by mitochondrial metabolic regulators. It has been proposed that defects in these pathways ultimately results in the development of fibrosis.[53,56] To support these findings, I showed that KBL409 administration improved defective energy metabolic pathways by restoring metabolic regulators and mitochondrial integrity, thus reducing fibrotic injury in CKD model.

A precise balance between fusion and fission is essential for mitochondrial fitness because defective mitochondrial dynamics can cause mitochondrial dysfunction and cell apoptosis.[57] Studies with rodent and human diabetic kidneys have unveiled enhanced fragmentation of mitochondria in the kidney TECs and podocytes.[5,19,58] In addition, the conditional knockdown of *Drp1*, an essential component of mitochondrial fission, or pharmacological inhibition of *Drp1* using Mdivi-1 significantly blunted mitochondrial fission and protected against the progression of diabetic nephropathy.[19] These findings indicate a causal link between the disruption of mitochondrial dynamics and kidney injury. Consistent with the results of previous studies, my study revealed a shift in mitochondrial dynamics toward fission in an adenine-induced CKD model. In addition, KBL409 administration restored the altered expression of mitochondrial dynamics-related genes and improved mitochondrial morphology and function. Taken together, these results suggest that KBL409 may exert renoprotective effects by restoring alterations of mitochondrial dynamics leading to better mitochondrial fitness in the context of kidney failure.

KBL409 may protect mitochondria in the kidney by increasing production of

연세대학교
YONSEI UNIVERSITY

beneficial SCFAs. SCFAs, including butyrate, acetate, and propionate, are a subgroup of fatty acids produced by the bacterial fermentation of complex carbohydrates and fiber in the large intestine. One of the hallmarks of dysbiosis in patients with CKD is the depletion of SCFA-producing bacteria.[59] Animal studies have demonstrated that administering probiotics of *Lactobacillus* species, including *Lactobacillus acidophilus*, increases fecal butyrate production by modulating gut microbiota.[60-62] *Lactobacillus acidophilus* also stimulates monocarboxylate transporter 1-mediated butyrate uptake and counteracts *E. coli*-induced inhibition of monocarboxylate transporter 1 function.[63] In addition, *Lactobacillus acidophilus* could produce acetate.[64] In line with previous studies, my study showed that KBL409 supplementation restored fecal concentrations of butyrate and acetate, which were significantly decreased in adenine-induced CKD mice compared with control mice. Of note, SCFAs have been reported to protect against mitochondrial stress in kidney and other types of cells. For instance, acetate treatment significantly diminishes inflammation and increases mtDNA contents in kidney tissues undergoing ischemia-reperfusion injury, most likely by modulating epigenetic processes.[23] In addition, butyrate improves mitochondrial biogenesis by promoting AMPK-PGC-1α and blocking the histone deacetylase signaling pathway in high-insulin induced hepatocytes.[65] Furthermore, butyrate and acetate also enhances mitochondrial repair by inducing mitochondrial dynamics to shift toward fusion in liver and pancreatic cells.[32,35] Consistent with these studies, my *in vitro* study demonstrated that butyrate restored alterations in mitochondrial dynamics, metabolism, respiration, and ATP generation in TECs under uremic conditions. Therefore, the protective effect of KBL409 on mitochondria shown in this study is likely mediated by SCFAs.

연세대학교
YONSEI UNIVERSITY

V. CONCLUSION

In conclusion, this study demonstrated that *Lactobacillus acidophilus* KBL409 supplementation reduced kidney fibrosis in an animal model of CKD. These favorable effects were mediated by mitochondrial fitness as evidenced by significant improvement in mitochondrial biogenesis, dynamics, metabolism, respiration, and ATP generation. These findings provide new insights into how probiotics promote mitochondrial function and that improving dysbiosis with probiotics may be a therapeutic option for delaying the progression of kidney disease.

연세대학교
YONSEI UNIVERSITY

REFERENCES

1. Wang Z, Ying Z, Bosy-Westphal A, Zhang J, Schautz B, Later W, et al. Specific metabolic rates of major organs and tissues across adulthood: evaluation by mechanistic model of resting energy expenditure. Am J Clin Nutr 2010;92:1369-1377.
2. Bhargava P, Schnellmann RG. Mitochondrial energetics in the kidney. Nat Rev Nephrol 2017;13:629-646.
3. Che R, Yuan Y, Huang S, Zhang A. Mitochondrial dysfunction in the pathophysiology of renal diseases. Am J Physiol Renal Physiol 2014;306:F367-378.
4. Galvan DL, Green NH, Danesh FR. The hallmarks of mitochondrial dysfunction in chronic kidney disease. Kidney Int 2017;92:1051-1057.
5. Coughlan MT, Nguyen TV, Penfold SA, Higgins GC, Thallas-Bonke V, Tan SM, et al. Mapping time-course mitochondrial adaptations in the kidney in experimental diabetes. Clin Sci (Lond) 2016;130:711-720.
6. Sharma K, Karl B, Mathew AV, Gangoiti JA, Wassel CL, Saito R, et al. Metabolomics reveals signature of mitochondrial dysfunction in diabetic kidney disease. J Am Soc Nephrol 2013;24:1901-1912.
7. Forbes JM, Thorburn DR. Mitochondrial dysfunction in diabetic kidney disease. Nat Rev Nephrol 2018;14:291-312.
8. Zhan M, Brooks C, Liu FY, Sun L, Dong Z. Mitochondrial dynamics: regulatory mechanisms and emerging role in renal pathophysiology. Kidney Int 2013;83:568-581.
9. Tang C, Cai J, Dong Z. Mitochondrial dysfunction in obesity-related kidney disease: a novel therapeutic target. Kidney Int 2016;90:930-933.
10. Szeto HH. Pharmacologic Approaches to Improve Mitochondrial Function in AKI and CKD. J Am Soc Nephrol 2017;28:2856-2865.
11. Bhatia D, Capili A, Choi ME. Mitochondrial dysfunction in kidney injury,

연세대학교
YONSEI UNIVERSITY

inflammation, and disease: Potential therapeutic approaches. Kidney Res Clin Pract 2020;39:244-258.

12. Dare AJ, Bolton EA, Pettigrew GJ, Bradley JA, Saeb-Parsy K, Murphy MP. Protection against renal ischemia-reperfusion injury in vivo by the mitochondria targeted antioxidant MitoQ. Redox Biol 2015;5:163-168.
13. Patil NK, Parajuli N, MacMillan-Crow LA, Mayeux PR. Inactivation of renal mitochondrial respiratory complexes and manganese superoxide dismutase during sepsis: mitochondria-targeted antioxidant mitigates injury. Am J Physiol Renal Physiol 2014;306:F734-743.
14. Mizuguchi Y, Chen J, Seshan SV, Poppas DP, Szeto HH, Felsen D. A novel cell-permeable antioxidant peptide decreases renal tubular apoptosis and damage in unilateral ureteral obstruction. Am J Physiol Renal Physiol 2008;295:F1545-1553.
15. Sohn M, Kim K, Uddin MJ, Lee G, Hwang I, Kang H, et al. Delayed treatment with fenofibrate protects against high-fat diet-induced kidney injury in mice: the possible role of AMPK autophagy. Am J Physiol Renal Physiol 2017;312:F323-F334.
16. Park CW, Zhang Y, Zhang X, Wu J, Chen L, Cha DR, et al. PPARalpha agonist fenofibrate improves diabetic nephropathy in db/db mice. Kidney Int 2006;69:1511-1517.
17. Yang HC, Deleuze S, Zuo Y, Potthoff SA, Ma LJ, Fogo AB. The PPARgamma agonist pioglitazone ameliorates aging-related progressive renal injury. J Am Soc Nephrol 2009;20:2380-2388.
18. Jesinkey SR, Funk JA, Stallons LJ, Wills LP, Megyesi JK, Beeson CC, et al. Formoterol restores mitochondrial and renal function after ischemia-reperfusion injury. J Am Soc Nephrol 2014;25:1157-1162.
19. Ayanga BA, Badal SS, Wang Y, Galvan DL, Chang BH, Schumacker PT, et al. Dynamin-Related Protein 1 Deficiency Improves Mitochondrial Fitness and

연세대학교
YONSEI UNIVERSITY

Protects against Progression of Diabetic Nephropathy. J Am Soc Nephrol 2016;27:2733-2747.

20. Jandhyala SM, Talukdar R, Subramanyam C, Vuyyuru H, Sasikala M, Nageshwar Reddy D. Role of the normal gut microbiota. World J Gastroenterol 2015;21:8787-8803.
21. Koppe L, Mafra D, Fouque D. Probiotics and chronic kidney disease. Kidney Int 2015;88:958-966.
22. Lau WL, Savoj J, Nakata MB, Vaziri ND. Altered microbiome in chronic kidney disease: systemic effects of gut-derived uremic toxins. Clin Sci (Lond) 2018;132:509-522.
23. Andrade-Oliveira V, Amano MT, Correa-Costa M, Castoldi A, Felizardo RJ, de Almeida DC, et al. Gut Bacteria Products Prevent AKI Induced by Ischemia-Reperfusion. J Am Soc Nephrol 2015;26:1877-1888.
24. Yang J, Lim SY, Ko YS, Lee HY, Oh SW, Kim MG, et al. Intestinal barrier disruption and dysregulated mucosal immunity contribute to kidney fibrosis in chronic kidney disease. Nephrol Dial Transplant 2019;34:419-428.
25. Iwashita Y, Ohya M, Yashiro M, Sonou T, Kawakami K, Nakashima Y, et al. Dietary Changes Involving Bifidobacterium longum and Other Nutrients Delays Chronic Kidney Disease Progression. Am J Nephrol 2018;47:325-332.
26. Yoshifuji A, Wakino S, Irie J, Tajima T, Hasegawa K, Kanda T, et al. Gut Lactobacillus protects against the progression of renal damage by modulating the gut environment in rats. Nephrol Dial Transplant 2016;31:401-412.
27. Wei M, Wang Z, Liu H, Jiang H, Wang M, Liang S, et al. Probiotic Bifidobacterium animalis subsp. lactis Bi-07 alleviates bacterial translocation and ameliorates microinflammation in experimental uraemia. Nephrology (Carlton) 2014;19:500-506.
28. Xia B, Yu J, He T, Liu X, Su J, Wang M, et al. Lactobacillus johnsonii L531 ameliorates enteritis via elimination of damaged mitochondria and suppression of

연세대학교
YONSEI UNIVERSITY

SQSTM1-dependent mitophagy in a Salmonella infantis model of piglet diarrhea. FASEB J 2020;34:2821-2839.

29. Tunapong W, Apaijai N, Yasom S, Tanajak P, Wanchai K, Chunchai T, et al. Chronic treatment with prebiotics, probiotics and synbiotics attenuated cardiac dysfunction by improving cardiac mitochondrial dysfunction in male obese insulin-resistant rats. Eur J Nutr 2018;57:2091-2104.
30. d'Ettorre G, Rossi G, Scagnolari C, Andreotti M, Giustini N, Serafino S, et al. Probiotic supplementation promotes a reduction in T-cell activation, an increase in Th17 frequencies, and a recovery of intestinal epithelium integrity and mitochondrial morphology in ART-treated HIV-1-positive patients. Immun Inflamm Dis 2017;5:244-260.
31. Ren T, Zhu L, Shen Y, Mou Q, Lin T, Feng H. Protection of hepatocyte mitochondrial function by blueberry juice and probiotics via SIRT1 regulation in non-alcoholic fatty liver disease. Food Funct 2019;10:1540-1551.
32. Mollica MP, Mattace Raso G, Cavaliere G, Trinchese G, De Filippo C, Aceto S, et al. Butyrate Regulates Liver Mitochondrial Function, Efficiency, and Dynamics in Insulin-Resistant Obese Mice. Diabetes 2017;66:1405-1418.
33. Gao Z, Yin J, Zhang J, Ward RE, Martin RJ, Lefevre M, et al. Butyrate improves insulin sensitivity and increases energy expenditure in mice. Diabetes 2009;58:1509-1517.
34. Hu J, Kyrou I, Tan BK, Dimitriadis GK, Ramanjaneya M, Tripathi G, et al. Short-Chain Fatty Acid Acetate Stimulates Adipogenesis and Mitochondrial Biogenesis via GPR43 in Brown Adipocytes. Endocrinology 2016;157:1881-1894.
35. Hu S, Kuwabara R, de Haan BJ, Smink AM, de Vos P. Acetate and Butyrate Improve β-cell Metabolism and Mitochondrial Respiration under Oxidative Stress. Int J Mol Sci 2020;21.
36. Kim H. Lactobacillus acidophilus KBL409 reduced kidney fibrosis via immune

연세대학교
YONSEI UNIVERSITY

modulatory effects in mice with chronic kidney disease[dissertation]. Yonsei Univ.; 2021.

37. Diwan V, Brown L, Gobe GC. Adenine-induced chronic kidney disease in rats. Nephrology (Carlton) 2018;23:5-11.
38. Nangaku M, Pippin J, Couser WG. Complement membrane attack complex (C5b-9) mediates interstitial disease in experimental nephrotic syndrome. J Am Soc Nephrol 1999;10:2323-2331.
39. Vaziri ND, Wong J, Pahl M, Piceno YM, Yuan J, DeSantis TZ, et al. Chronic kidney disease alters intestinal microbial flora. Kidney Int 2013;83:308-315.
40. Vaziri ND, Yuan J, Rahimi A, Ni Z, Said H, Subramanian VS. Disintegration of colonic epithelial tight junction in uremia: a likely cause of CKD-associated inflammation. Nephrol Dial Transplant 2012;27:2686-2693.
41. Andersen K, Kesper MS, Marschner JA, Konrad L, Ryu M, Kumar Vr S, et al. Intestinal Dysbiosis, Barrier Dysfunction, and Bacterial Translocation Account for CKD-Related Systemic Inflammation. J Am Soc Nephrol 2017;28:76-83.
42. Miranda Alatriste PV, Urbina Arronte R, Gomez Espinosa CO, Espinosa Cuevas Mde L. Effect of probiotics on human blood urea levels in patients with chronic renal failure. Nutr Hosp 2014;29:582-590.
43. Natarajan R, Pechenyak B, Vyas U, Ranganathan P, Weinberg A, Liang P, et al. Randomized controlled trial of strain-specific probiotic formulation (Renadyl) in dialysis patients. Biomed Res Int 2014;2014:568571.
44. Rossi M, Johnson DW, Morrison M, Pascoe EM, Coombes JS, Forbes JM, et al. Synbiotics Easing Renal Failure by Improving Gut Microbiology (SYNERGY): A Randomized Trial. Clin J Am Soc Nephrol 2016;11:223-231.
45. Borges NA, Carmo FL, Stockler-Pinto MB, de Brito JS, Dolenga CJ, Ferreira DC, et al. Probiotic Supplementation in Chronic Kidney Disease: A Double-blind, Randomized, Placebo-controlled Trial. J Ren Nutr 2018;28:28-36.
46. Eidi F, Poor-Reza Gholi F, Ostadrahimi A, Dalili N, Samadian F, Barzegari A.

연세대학교
YONSEI UNIVERSITY

Effect of Lactobacillus Rhamnosus on serum uremic toxins (phenol and P-Cresol) in hemodialysis patients: A double blind randomized clinical trial. Clin Nutr ESPEN 2018;28:158-164.

47. Borges NA, Stenvinkel P, Bergman P, Qureshi AR, Lindholm B, Moraes C, et al. Effects of Probiotic Supplementation on Trimethylamine-N-Oxide Plasma Levels in Hemodialysis Patients: a Pilot Study. Probiotics Antimicrob Proteins 2019;11:648-654.
48. Lopes R, Theodoro JMV, da Silva BP, Queiroz VAV, de Castro Moreira ME, Mantovani HC, et al. Synbiotic meal decreases uremic toxins in hemodialysis individuals: A placebo-controlled trial. Food Res Int 2019;116:241-248.
49. Fontecha-Barriuso M, Martin-Sanchez D, Martinez-Moreno JM, Monsalve M, Ramos AM, Sanchez-Nino MD, et al. The Role of PGC-1alpha and Mitochondrial Biogenesis in Kidney Diseases. Biomolecules 2020;10.
50. Hong Q, Zhang L, Das B, Li Z, Liu B, Cai G, et al. Increased podocyte Sirtuin-1 function attenuates diabetic kidney injury. Kidney Int 2018;93:1330-1343.
51. Zhang T, Chi Y, Kang Y, Lu H, Niu H, Liu W, et al. Resveratrol ameliorates podocyte damage in diabetic mice via SIRT1/PGC-1α mediated attenuation of mitochondrial oxidative stress. J Cell Physiol 2019;234:5033-5043.
52. Kim MY, Lim JH, Youn HH, Hong YA, Yang KS, Park HS, et al. Resveratrol prevents renal lipotoxicity and inhibits mesangial cell glucotoxicity in a manner dependent on the AMPK-SIRT1-PGC1alpha axis in db/db mice. Diabetologia 2013;56:204-217.
53. Kang HM, Ahn SH, Choi P, Ko YA, Han SH, Chinga F, et al. Defective fatty acid oxidation in renal tubular epithelial cells has a key role in kidney fibrosis development. Nat Med 2015;21:37-46.
54. Han SH, Wu MY, Nam BY, Park JT, Yoo TH, Kang SW, et al. PGC-1alpha Protects from Notch-Induced Kidney Fibrosis Development. J Am Soc Nephrol 2017;28:3312-3322.

연세대학교
YONSEI UNIVERSITY

55. Nam BY, Jhee JH, Park J, Kim S, Kim G, Park JT, et al. PGC-1alpha inhibits the NLRP3 inflammasome via preserving mitochondrial viability to protect kidney fibrosis. Cell Death Dis 2022;13:31.
56. Chung KW, Lee EK, Lee MK, Oh GT, Yu BP, Chung HY. Impairment of PPARalpha and the Fatty Acid Oxidation Pathway Aggravates Renal Fibrosis during Aging. J Am Soc Nephrol 2018;29:1223-1237.
57. Brooks C, Cho SG, Wang CY, Yang T, Dong Z. Fragmented mitochondria are sensitized to Bax insertion and activation during apoptosis. Am J Physiol Cell Physiol 2011;300:C447-455.
58. Zhan M, Usman IM, Sun L, Kanwar YS. Disruption of renal tubular mitochondrial quality control by Myo-inositol oxygenase in diabetic kidney disease. J Am Soc Nephrol 2015;26:1304-1321.
59. Wong J, Piceno YM, DeSantis TZ, Pahl M, Andersen GL, Vaziri ND. Expansion of urease- and uricase-containing, indole- and p-cresol-forming and contraction of short-chain fatty acid-producing intestinal microbiota in ESRD. Am J Nephrol 2014;39:230-237.
60. Vemuri R, Martoni CJ, Kavanagh K, Eri R. Lactobacillus acidophilus DDS-1 Modulates the Gut Microbial Co-Occurrence Networks in Aging Mice. Nutrients 2022;14.
61. Wang JJ, Zhang QM, Ni WW, Zhang X, Li Y, Li AL, et al. Modulatory effect of Lactobacillus acidophilus KLDS 1.0738 on intestinal short-chain fatty acids metabolism and GPR41/43 expression in beta-lactoglobulin-sensitized mice. Microbiol Immunol 2019;63:303-315.
62. Berni Canani R, Sangwan N, Stefka AT, Nocerino R, Paparo L, Aitoro R, et al. Lactobacillus rhamnosus GG-supplemented formula expands butyrate-producing bacterial strains in food allergic infants. ISME J 2016;10:742-750.
63. Kumar A, Alrefai WA, Borthakur A, Dudeja PK. Lactobacillus acidophilus counteracts enteropathogenic E. coli-induced inhibition of butyrate uptake in

연세대학교
YONSEI UNIVERSITY

intestinal epithelial cells. Am J Physiol Gastrointest Liver Physiol 2015;309:G602-607.

64. Wang MX, Lin L, Chen YD, Zhong YP, Lin YX, Li P, et al. Evodiamine has therapeutic efficacy in ulcerative colitis by increasing Lactobacillus acidophilus levels and acetate production. Pharmacol Res 2020;159:104978.

65. Zhao T, Gu J, Zhang H, Wang Z, Zhang W, Zhao Y, et al. Sodium Butyrate-Modulated Mitochondrial Function in High-Insulin Induced HepG2 Cell Dysfunction. Oxid Med Cell Longev 2020;2020:1904609.

연세대학교
YONSEI UNIVERSITY

ABSTRACT (IN KOREAN)

만성콩팥병 동물 모델에서 *Lactobacillus acidophilus* KBL409의 미토콘드리아 기능 향상에 의한 신장 보호 효과

<지도교수 한승혁>

연세대학교 대학원 의학과

남기헌

배경: 미토콘드리아 기능 장애는 만성콩팥병의 진행에 중요한 역할을 하는 것으로 알려졌다. 또한, 최근 들어 장내 미생물 불균형이 만성콩팥병의 발병과 연관이 있다는 것이 밝혀지고 있다. 이 연구는 만성콩팥병 동물 모델에서 프로바이오틱스의 미토콘드리아 기능 개선을 통한 신장 손상에 대한 보호효과를 평가하고자 하였다.

방법: 만성콩팥병 동물 모델은 C57BL/6 쥐에게 0.2% 아데닌을 함유한 식이를 공급하여 유도하였다. *Lactobacillus acidophilus* KBL409를 이 쥐에게 3주 동안 매일 1×10^9 CFU의 용량으로 경구 투여하였다. 체외 실험으로 KBL409의 미토콘드리아 보호 기전을 확인하기 위해 쥐로부터 직접 얻은 세뇨관 상피 세포를 일차배양하여 TGF-β 및 p-cresyl sulfate로 자극하고 단쇄지방산(butyrate)을 함께 투여하였다.

결과: 만성콩팥병이 유도된 쥐는 대조군에 비해 PGC-1α와 AMPK의 발현이 감소하였으며, 미토콘드리아의 분열의 증가와 미토콘드리아 질량의 감소 소견을 보였다. 그러나 KBL409 투여로 이러한 변화가 호전됨을 관찰하였다. KBL409 투여는 만성콩팥병이 유도된 쥐의 지방산 산화 및 포도당 분해 과정의 결함을 개선하였으며, TCA 회로와 관련된 효소의 발현을 향상시켰다. 나아가 KBL409 투여로 미토콘드리아 기능 분석에 의해 평가된 미토콘드리아 호흡 및 ATP 생산의 개선을 확인하였다. KBL409의 미토콘드리아 보호 효과로

연세대학교
YONSEI UNIVERSITY

만성콩팥병 쥐의 섬유화 관련 인자들의 발현이 감소하고, 신장 조직에서 섬유화가 감소함을 확인하였다. 체외 실험에서 TGF-β 및 p-cresyl sulfate로 자극한 세뇨관 상피세포에서 동물 실험과 동일한 결과를 확인하였다.

결론: 이상의 결과를 통해 프로바이오틱스 KBL409 투여가 만성콩팥병에서 미토콘드리아 보호 효과를 통해 신장 손상의 진행을 억제시킬 수 있다는 것을 확인하였다.

핵심되는 말: 프로바이오틱스, KBL409, 미토콘드리아, 만성콩팥병